Master's thesis

NTNU
Norwegian University of Science and Technology
Faculty of Engineering
Department of Civil and Environmental Engineering

Kristine Bergseng

Performance of closed particle removal systems for treatment of road runoff

Master's thesis in Water Supply and Wastewater Engineering
Supervisor: Tone Merete Muthanna
July 2021

NTNU
Norwegian University of
Science and Technology

Kristine Bergseng

Performance of closed particle removal systems for treatment of road runoff

Master's thesis in Water Supply and Wastewater Engineering
Supervisor: Tone Merete Muthanna
July 2021

Norwegian University of Science and Technology
Faculty of Engineering
Department of Civil and Environmental Engineering

NTNU
Norwegian University of
Science and Technology

Preface

This work has been carried out in the spring of 2021 as the final product in the course TVM4905 Water Supply and Wastewater Systems, Master's Thesis at the Norweian University of Science and Technology (NTNU), Department of Civil and Environmental Engineering (DCEE). The thesis is written as scientific paper and is planned to be submitted to a scientific journal. The aim of the master's project was to investigate the particle removal efficiency of a hydrodynamic vortex separator (HVS) and a modular sedimentation system (MSS). Field work was conducted at the two sites followed by laboratory work in the analytical laboratory and hydraulic research hall at the department. In addition some water samples were digested and prepared at the Department of Chemistry, NTNU, before metal analyses was conducted by SINTEF Industy. Parallel to the field and lab work a runoff model was created and calibrated for the upstream system of the HVS. The work at the HVS is a continuation of the master's theisis by Merethe Arntsen Strømberg in the spring of 2020 with the title "Sediment removal performance of a hydrodynamic vortex separator".

I would like to thank my supervisor Professor Tone Merete Muthanna for giving me advice throughout the work. The competence and engagement shown in the project and process of writing has been truly inspiring. A special thank you goes to my helpful boyfriend, Sivert Heidsve, for coming with me doing field work at the HVS both early in the morning and late at night adding up to a total of 37 times. I am very thankful for all the help and support you have provided throughout the master's period. Also, thanks to:

- Lars and Per Møller-Pedersen for giving me an introduction to the MSS. Special thanks to Lars Møller-Pedersen for helping with the sampling and sending the water samples fast to Trondheim. The study of the MSS would not be possible without this help.
- Trine Håberg Næsss, DCEE, NTNU, for all training, kindness, determination, and help in the analytical laboratory. A special thanks for the teamwork while using the UltraCLAVE.
- Merethe Arntsen Strømberg, Norconsult, for the introduction to the study site at the HVS, academic discussion and help with performing the sediment analyses.
- Elhadi Mohsen Hassan Abdalla, DCEE, NTNU, for giving me an introduction to R and helping me with the calibration script.
- Vincent Pons, DCEE, NTNU, for the discussion regarding calibration data.
- Anica Simic, Department of Chemistry, NTNU, for letting me use the UltraCLAVE.
- Marianne Steinsvik Kjos, SINTEF Industry, for performing metal analyses.
- The Norwegian Public Roads Administration, Trondheim Municipality and Klima 2050 for the collaboration.
- Christoffer Kjelsberg, Veidekke, and Hans Olav Børseth, Norske Voav-Teknikk A/S, for the safety and help when taking sediment samples upstream the HVS at E6.
- Sofie Eivik Karlsen, my friend, for all academic discussion, laughter and support.

Trondheim, 12th of July 2021

Kristine Bergseng

Sammendrag

Verda over, inkludert i Noreg, gjev klimaendringar uføreseielege nedbørmønster og -mengder. Dette har resultert i ein tre-trinnsstrategi for overflatevatn. Steg ein dreidde seg originalt om den lokale vassbalansen, trinn to om fordrøyning av vatn ved større avrenningshendingar og trinn tre om å sikre trygge flomvegar. Hyppigare ekstreme avrenningshendingar har ført til eit stort fokus på avrenningsmengder og -volum over dei siste tiåra. I dette vert fokuset på vasskvalitet forsømt. Fokuset på vassmengder har ført til store dimensjonar på vasskvalitet-sløysingar, som har resultert i svekket reinseevne i nokon tilfelle samt dyre løysingar.

Denne studien har sett på to typar vegavrenningsreinseløysningar ved høvesvis E6 i Trondheim og Fv 505 i Sandnes. Det vert teken vassprøvar i innløp og utløp ved fleire avrenningshendingar i eit supersandfang og eit undergrunns sedimentasjonssystem. Automatiske prøvetakarar tok prøver over lengre tid i kvar avrenningshendig, slik at utviklinga gjennom hendinga vart funne. Vassprøvene vert analysert for totalt suspendert stoff, partikkelstørrelsefordeling og utvalde metall. Metallkonsentrasjonane for Ni, Cu, Zn, Cd og Pb vart bestemd for tre ulike fraksjonar: grove partiklar, fine partiklar og laust stoff.

Reinseeffektiviteten av total suspendert stoff for supersandfanget varierte frå 10 til 40 %, imens sedimentasjonssystemet oppnådde ein reinsegrad frå 48 til over 98 %. Partikkelstørrelsefordelinga varierte mellom dei to anlegga, men i begge var over 90 % av partiklane i antal mindre enn 1 μm. Metallfjerninga varierte over element og fraksjon. Funn i denne studien framhevar viktigheita av partikkelkarakterisering av vegvatnet når ein dimensjonerer partikkelfjerningsanlegg.

Table of contents

List of Figures

List of Tables

Abbreviations

AA-EQS	Annual average environmental quality standard
AADT	Annual average daily traffic
AV	Area velocity
DIS	Sediment sample analyzed with dispersant
E6	Europavei 6
EC	Electrical conductivity
EQS	Environmental quality standards
Fv 505	Fylkesvei 505
HVS	Hydrodynamic vortex separator
MSS	Modular Sedimentation System
NAT	Sediment sample analyzed without dipersant
NPRA	Norwegian Public Roads Administration.*Nor: Statens Vegvesen*
NTNU	Norwegian University of Science and Technology
PNEC	Predicted no effect concentration
PSD	Particle size distribution
SWMM	Storm Water Management Model
TSS	Total suspended solids
Turb	Turbidity

Performance of closed particle removal systems for treatment of road runoff

Kristine Bergseng

Department of Civil and Environmental Engineering
Norwegian University of Science and Technology

1 Abstract

Changes in the global climate are causing major challenges resulting in unpredictability in precipitation amounts and patterns worldwide, including Norway. This has resulted in a three-step approach for surface runoff water. Step one originally included local water balance, step two flood detention, and step three safe floodways. The more frequent extreme events have led to a focus on runoff quantities and volumes for flood detention over the last decades, neglecting the water quality considerations. The early focus on quantity has resulted in large designs of treatment facilities, causing impaired treatment performance and more expensive measures.

This study investigates two types of road runoff treatment measures located in two coastal cities in Norway. One hydrodynamic vortex separator (HVS) and one underground modular sedimentation system (MSS) were monitored using automatic samplers to collect water samples in the inflow and outflow of the treatment facilities. The samples were analyzed for total suspended solids, particle size distribution (PSD), and selected heavy metals. Metal concentrations for Ni, Cu, Zn, Cd, and Pb were determined for three fractions; coarse particle, fine particle, and dissolved.

The sediment removal efficiency at the HVS ranged from 10 to 40 %, while the MSS achieved particle removal of 48 to over 98 %. Particle size distribution differed, but over 90 % of all particles were below 1 μm. Metal removal variated over element and fraction. Findings in this study accentuate the importance of particle characterization of the road runoff when designing a treatment facilities.

Keywords: Three-step approach; Treatment efficiency; Road runoff; Particle size distribution; Heavy metals

2 Introduction

Traditionally the approach for managing surface runoff has been to convey water away from the road surface using piped systems. In Norway, climate change has led to more frequent heavy rainfall events. In combination with urbanization, this has resulted in capacity problems in these exciting systems, causing damage to buildings and infrastructure (Sorteberg et al., 2018). To alleviate this problem, stormwater management has taken on a volume-based focus. This focus, coupled with the introduction of climate factors in design, has resulted in solutions with large hydraulic capacities. Management of the water resources as a whole has revealed that stormwater can cause significant negative consequences in receiving water bodies (Hoffman et al., 1985; Viklander et al., 2003; among others). Stormwater contain multiple pollutants from metals to organics and micropollutants at varying concentrations and loads (Tsihrintzis and Hamid, 1997; Makepeace et al., 1995). Road runoff is among the most contaminated sources of stormwater where depositions from road salt, anti-skid agents, emissions from vehicles, wear from tiers, vehicle parts, and pavements are present (Marsalek et al., 2003).

Lindholm et al. (2008) introduced the three-step approach to meet the challenges of a changing climate. The three-step approach is a volume-oriented approach differentiated based on small, medium, and large precipitation events. The design criteria for stormwater pipes are a 20-year return period, which has become the standard by practice also for step one solutions. Standard return periods for step two and three have been 20 to 200-year events, dependent on downstream infrastructure. Additionally, local norms impose climate factors for precaution reasons. Paus (2018) has analyzed precipitation data and suggests a design value for step one at 95 % of the annual precipitation, which typically corresponds to two-thirds of the two-year rain. This is an commonly used design value internationally (Shrestha et al., 2014). The initial step one approach emphasizes infiltration of small rain events, but the step has evolved to concern the improvement of water quality (Paus, 2018). However, the volume oriented approach has led to design of water quality measures with a large hydraulic loading capacity, that for some are reducing treatment efficiency because it is not optimized for everyday events.

Construction and operation of roads may cause negative impacts on the aquatic environment (Viklander et al., 2003; Marsalek et al., 2005). The EU's Water Framework Directive aims to ensure a good ecological and chemical status for ground and surface water. It is implemented in Norwegian law through the Water Regulation (Vanndirektivet). The Norwegian Public Roads Administration (NPRA) handbook N200 implements these regulations in road design. Requirements in the N200 handbook are based on the vulnerability of the receiving water body and the annual average daily traffic (AADT) on the road. There are two treatment requirements. The first focuses on removing particular matter, and the second one targets dissolved pollutants. However, low AADT ($<$3000) exempt from treatment. The Water Framework Directive defines 45 priority substances, which have environmental quality standards (EQS) given as threshold values between good and bad ecological state. These are given as yearly average and maximum concentrations for the water body. However, these become difficult to relate to when designing a treatment measure due to the typical low volume of the road runoff compared to the recipient. Treatment requirements are clearly stating *when*

treatment is required, but neither clear targets for percentage removal nor concentration limits are specified. Meland (2010), documented that road runoff has the potential to disturb aquatic biota, even during episodes with a low concentration of pollutants. Many studies have been conducted on particles in stormwater, finding that many particles are present in the first flush of a runoff event (Cheng et al., 2017; Sansalone and Buchberger, 1997b; Li et al., 2005; among others).

Underground structures are popular measures to remove particles from road runoff in urban areas due to their small above-ground footprint. The devices divide into three groups: Filters, hydrodynamic vortex separators, and underground settling tanks (Wilson et al., 2009). The two latter have a primary function to remove suspended solids and floatables from the runoff. Settling tanks utilize sedimentation to remove particles (Li et al., 2006), while particles in the hydrodynamic vortex separators (HVS) separates from the flow by a swirl effect (Andoh and Saul, 2003). Aldheimer and Bennerstedt (2003), found an average 84 % removal of suspended solids in a settling tank treating highway runoff. Settling tanks remove particles larger than 100 μm effectively, while small particles need more specific designs that give a larger hydraulic residence time (Li et al., 2008). Treatment efficiencies of HVS are reported to vary widely (Lee et al., 2014; Strømberg, 2020; Tran and Kang, 2013; among others). The treatment efficiency is dependent on influent discharge and characteristics of particles (Sansalone and Pathapati, 2009; Butler and Karunaratne, 1995).

Particle size distribution (PSD) is important to characterize the particles in the system (Selbig et al., 2016). The particle size distributions from road runoff differ with spatial and temporal variations (Monrabal-Martinez et al., 2019; Kim and Sansalone, 2008; Strømberg, 2020; Westerlund and Viklander, 2006). Differences in sampling and analytical methods typically make PSD difficult to compare over different sites. Across studies a large portion of the metals are found to be particle-bound (Ball et al., 1998; Tuccillo, 2006; Viklander, 1998; among others), which makes particle removal an efficient way to hinder heavy metal pollution reaching the receiving the water body (Li et al., 2005). Especially smaller particles are important to remove, as these carry a larger bulk of metals, giving them a higher toxic effect (Wang et al., 1998; Li et al., 2005). Sartor et al. (1974), found that over 50 % of the heavy metals were associated with particles smaller than 43 μm, while this fraction only accounted for 5.9 % of the total solids by weight.

As the current design practice funds on the three-step approach developed to handle quantities, it points to the need to develop water quality-based design guidelines for the treatment of road runoff. The purpose of this study is to investigate the treatment efficiency of two selected systems: a hydrodynamic vortex separator and a modular settling system (MSS). The paper aims to answer the following research questions:

- What does water quality parameters (PSD, total suspended solids, and heavy metals) in the inflow and effluent of the hydrodynamic vortex separator and modular settling system indicate for the particle removal efficiency?
- What are the design implications for step one water quality treatment measures based on the findings in this study?

3 Materials and method

This section includes a description of the study sites, water sampling, and sediment sampling in the field. The laboratory analyses done on the water and sediment samples are outlined.

3.1 Description of study areas

The study sites include two road runoff treatment facilities; (1) a full-scale hydrodynamic vortex separator (HVS) located south of Trondheim treating runoff from the major highway E6 and (2) a modular closed settling tank south of Sandnes by the regional highway Fv505. Trondheim and Sandnes are coastal cities with cold (Dfc) and temperate (Cfb) climates according to the Köppen-Geiger climate classification (Beck et al., 2018), respectively. The sites differed in traffic intensity, with an AADT of 28 640 for E6 (NPRA, 2021a) compared to an AADT of 6 840 for Fv. 505 (NPRA, 2021b).

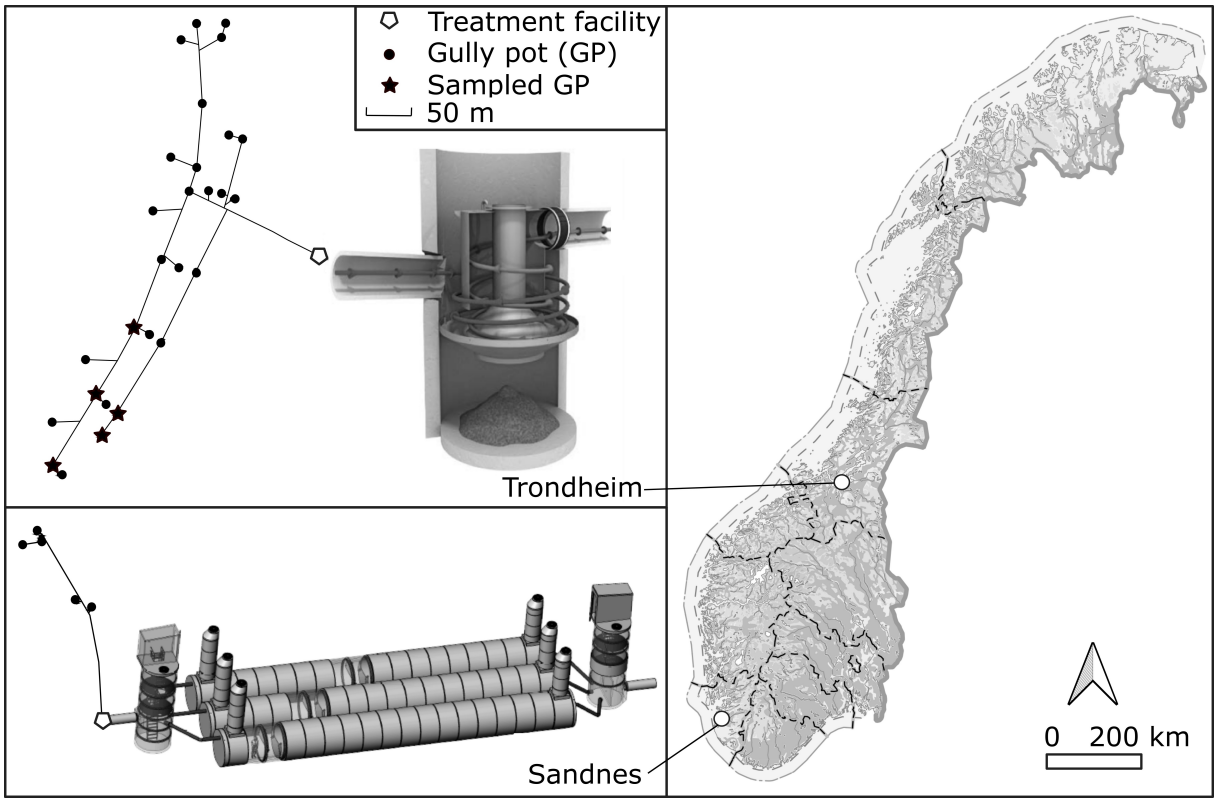

Figure 1: The location of the hydrodynamic vortex separator (HVS) and modular sedimentation system (MSS) with the upstream systems outlined. In the upper left corner, the HVS is illustrated with a figure from Hydro International (NJCAT Technology Verification, 2015), while in the lower corner, the MSS is shown with technical drawings from Skjæveland Cementstøperi AS. The map is retrieved from Kartverket (2021).

The total area of 47 ha is draining to the HVS, of which 12,3 ha are impervious road surface area, and the remaining 34.7 ha are grass-covered (Strømberg, 2020). The road runoff is conveyed in grass-covered swales into the nearest inlets. There is a total of 28 gully pots upstream of the HVS. The treatment of the road runoff, therefore, starts upstream the HVS in the swales (Fardel et al., 2019) and gully pots (Butler and Karunaratne, 1995). Directly upstream of the HVS, a 88 m^3 detention basin is located, followed by a flow regulator. The system is presented to the top left in Figure 1. A more detailed description of the system can be found in Strømberg (2020). The installed HVS is a Downstream Defender with an inner diameter of 2550 mm from Hydro International with a dimensioned flow of 192 L/s[1] and a maximum flow capacity of 270 L/s. However, the flow regulator restricts the inflow to 135 L/s, which is the permitted inflow to the downstream storm sewer. The inlet of the HVS generates a swirl in the chamber that directs the particles to settle into a sediment chamber with a storage capacity of 3.8 m^3. Oil and other floatables will be removed as it rises to the top.

An underground modular settling system (MSS) treats water from a catchment area of 1.44 ha with impervious four-lane road surface including a bridge and a roundabout as the significant land use (Storm Aqua AS, 2021). The road is expected to have a traffic 12 000 AADT in the future. The system is designed to remove particulate bound pollutants according to the NPRA's design handbook N200 (NPRA, 2018). The water enters the treatment facility into a modified manhole with a diameter of 2500 mm designed to remove coarse sediments, oil, and floatables. After the manhole, the water flows into one of three settling tanks, with a length of 26.5 m and a diameter of 2400 mm. Before the water leaves the treatment system, the water from all three tanks flows into the same gully pot. The facility can be seen to the bottom left in Figure 1.

3.2 Water samples

Teledyne ISCO automatic samplers were installed in the pipes of the manholes immediately upstream and downstream of the treatment facilities. At the HVS study site, the 6712 Portable Samplers with additional 750 Area Velocity (AV) Modules were used. The automatic samplers were mounted to the concrete wall under the manhole cover. Low-Profile Velocity Sensors were used with the AV module. The samples were collected through perforated polypropylene strainers with a diameter of 3.3 cm. At the MSS study site, 3700 Full-Size Portable Samplers were used. Due to the design of the system, it was not possible to use strainers. Therefore suction lines were mounted to the bottom of the inlet and outlet pipes. Pictures of the setup can be found in Appendix A.

The sampling procedure at the HVS was flow-triggered automatic sampling, while at the settling tank, it is according to NS-EN 16479:2014 constant time variable volume sampling. The reason for the different procedures was the available samplers, together with the access to power. The flow-triggered samplers were chosen to be placed at Tiller because of the fast response and the need to use batteries. The settling tank has a greater response time

1. Given in the Technical specifications and documentation from the supplier Miljø-og Fluidteknikk As (internal communication).

from the water entering to the water is leaving the facility. Consequently, it is found suitable to use a sampling program with constant time. Both of the procedures gave the possibility to sample the first flush and the entire runoff event. Manual sampling would not allow the same possibilities due to the time-extensiveness and the lack of flexibility. The automatic samplers at site one were programmed to sample the water when the AV sensors registered a pre-defined water level, which was high enough so the water could flow through the strainer. In the inflow sampling point of the HVS, the water level was set to 3.5 cm, while at the outflow it was slightly lower at 3.0 cm. The reason for different water levels is the detention of flow through the HVS and generally lower outflow. All samplers were programmed to collect 120 mL each sampling; in Trondheim, every five minutes as long as the water was over the pre-defined water level, while in Sandnes, the time between each sampling was set based on the weather forecast before each event started. Information about each sampling event are found in Table 1. All samplers have 24 polyethylene bottles of 500 mL, giving the capacity of sampling water 96 times. Each composite sample bottle consists of four single samples. This gave the opportunity to look at different fractions of the runoff event and the development over time. Inlet and outlet samples were paired together by finding the outlet sample closest in time from when the corresponding inlet sample was taken.

The samples were collected and brought to the lab as soon as the sampling was completed. According to Li et al. (2005) particles will start to aggregate after 6 hours. Therefore, the samples were endeavor analyzed in the laboratory within a short time frame. Samples from the MSS was shipped to the laboratory at the Norwegian University of Science and Technology (NTNU) with express delivery overnight.

An ECH20 ECRN-100 0.2 mm tipping bucket gauge was located by the HVS manhole to record the rainfall events. The EM50 Data collection system stored the data with a 5-minute resolution of the whole sampling period. Precipitation data from the MSS site was retrieved from the Norwegian Centre for Climate Services (NCCS, 2020) station SN44730 located 7 km north of the site. The station has a resolution of the precipitation data of 1 hour. Rainfall events were separated with at least 240 minutes of dry period.

3.2.1 Laboratory analysis

Analyses of particle size distribution (PSD), total suspended solids (TSS), pH, electrical conductivity (EC), and turbidity were performed in the Water Analysis Laboratory at the NTNU. Water samples were fractionated, and the total fraction was digested with UltraCLAVE at NTNU before being analyzed for heavy metals at SINTEF. Information about the number of analyzes preformed are found in Table 1.

A PSD was performed with a Beckman Coulter LS230, which gives the possibility to measure a range of particles from 0.04 to 2000 μm with two different methods. The first method illuminates the water samples, measuring the light intensity flux based on diffraction of the laser light. In the second method, the LS230 obtains particle size information in the range 0.04 to 0.4 μm using Polarization Intensity Differential Scattering (PIDS). Results of the PSD-analysis from the instrument can be given as differential distributions for volume, surface area, or number percentage (Beckman Coulter, 2011). In this study, the latter was reported.

Before each sample, the instrument was rinsed three times with de-ionized water and filled with de-ionized water as background liquid. The sample bottles were gently inverted in order to get a representative sample without bubbles. A sample size of 5 mL to 140 mL was added to obtain a PIDS between 45 - 55 %. All samples were analyzed in three runs with a duration of 90 seconds and a pumping speed of 50 %.

The road water was vacuum filtered through a pre-weighed cellulose nitrate membrane (Whatman NC45) filters with an average pore size of 0.45 μm to determine TSS. Procedures were done according to the standard NS-EN 872 (Standards Norway, 2005), but the method deviates from the standard since 1.2 μm glass fiber filters were not used. This is due to the main presence of smaller particles. After vacuum filtering, the filter is dried at 105 °C, before the filter was weighed after reaching equilibrium with the surrounding air.

In order to distinguish between the coarse particle, fine particle, colloidal, and truly dissolved metal fractions, a fractionation was carried out. However, in the literature there is not a clear standard of defining the different size ranges (Wang et al., 2003; Huerta-Diaz et al., 2007; Tuccillo, 2006). This results in overlapping fractions in studies, making them onerous to compare. Due to this, it is desirable to make a common practice to fractions to compare studies and gain a greater understanding of road runoff. In Appendix B a review of the fractionation methods across several studies in Scandinavia was conducted. The review concludes that it is suitable to define the fractionation thresholds as following for this project: particulate ($>$ 0.45 μm) and dissolved ($<$ 45 μm). The particulate fraction is further divided into coarse particles, greater than 1.2 μm, and fine particles in the range from 0.45 to 1.2 μm. In the dissolved fraction, colloidal matter is defined as the size from 3 kDa to 0.45 μm, while particle sizes under 3 kDa truly dissolved. The same division between the particulate and dissolved fraction is also used in the Water Regulation (Vannforskriften, 2006).

Due to the COVID-19 pandemic, the delivery time of 3 kDa filters was 10 months; consequently, it was not possible to fractionate within the dissolved fraction in this study. Syringe filters with an average pore size of 1.2 μm and 0.45 μm were used for the fractionation, with a cellulose acetate membrane (Whatman) and polyethersulfone membrane (VWR), respectively.

Among heavy metals, Nickel (Ni), Copper (Cu), Zinck (Zn), Cadmium (Cd), and Lead (Pb) were selected due to their presence in urban runoff at potential harmful concentrations (Direktoratsgruppen vanndiriktivet, 2018). Before the analysis, the samples were fractionated and preserved by adding five drops of ultrapure 0.1 M nitric acid (HNO_3) per 15 mL sample. The total metal samples were digested with UltraCLAVE from Milestone prior to analysis in the ICP-MS to get the sample in solution form. The UltraCLAVE digestion samples were prepared with 2 mL of water sample and 4 mL of ultrapure 65% HNO_3. The UltraCLAVE was done in a time period of 1t 18 min stepwise, increasing the temperature and pressure to 245°C and 205 bars under constant microwave power of 1000 W. Cooling was performed in the same reversed stepwise order. After digestion, the samples were diluted to 15 mL before metal analyses were conducted. Heavy metals were analyzed by an ICPQQQ, Agilent 8800 (Agilent Technologies) instrument externally at SINTEF Industry, Trondheim. The metal concentrations in the coarse particle and fine particle fractions were determined by subtracting the concentration of the 1.2 μm from the total concentration and the 0.45 μm filtrate from the 1.2 μm filtrate, respectively.

If the fraction came out as negative after subtraction, the fraction concentration was set as zero. In that case, the corresponding paired upstream or downstream metal concentration (n) was added to sample $n+1$. The 0.45 μm filtrate gave the metal concentration of the dissolved fraction.

The percentage removal efficiency of TSS and metals for the treatment facilities were found using equation 1, with the average inflow and outflow concentrations of each event.

$$\text{Removal efficiency}[\%] = \frac{\text{Inflow concentration - Outflow concentration}}{\text{Inflow concentration}} * 100 \qquad (1)$$

3.3 Runoff modeling

A rainfall-runoff simulation model was developed in Storm Water Management Model (SWMM) (EPA, 2020) for the study site in Trondheim in order to estimate the flow into the HVS. The runoff coefficient was set for each sub-catchment based on the land use, where 0.95 was used for the road and 0.6 for the grass-covered areas. The model was based on the catchment characteristics and pipe information from Strømberg (2020) and internal technical drawings of the cite from the NPRA. Manhole depths are not included for the system upstream of the detention basin. The slope of the pipes was assumed to be equal to the surface gradient. The Kinematic Wave and Horton equation were chosen as routing and infiltration models, respectively. The roughness of the pipes was set to a Manning's value of 0.012 (Table A.7, Rossman (2015)). Additional model parameters are given in Appendix C.

To calibrate the model, Micro-Divers (Diameter = 18 mm) from Van Essen were installed in the inflow pipe of the upstream manhole of the HVS. A Baro-Diver was hung next to the ECH20 gauge to compensate the Micro-Divers for atmospheric pressure. The divers logged data from April 16 to May 13. The model was calibrated with diver data and precipitation recorded in the period between April 21st and May 13th using R-studio with R version 3.6.1 (RStudio Team, 2019). The calibrated parameters were Mannings n for impervious and pervious surfaces. The R-script, found in Appendix C, used a differential evaluation method to optimize the parameters with the Nash Sutcliffe model efficiency, which aims to evaluate the peak performance. In order to find the 95 % value of the yearly flow, 30 years of precipitation data from Risvollan with one-minute resolution from the 25th of January 1989 to the 31st of December 2019 (retrieved from NCCS (2020), station SN68230), was used as input data for the calibrated model.

Table 1: Information about sampling the sampling program and lab analyzes performed on the samples from each rain event. Data from both the hydrodynamic vortex separator (HVS) and modular settling system (MSS) are each presented in the table. Due to insufficient amounts and/or the number of particles in the water, all analyzes, particle size distribution (PSD), pH, electrical conductivity (EC), Turbidity (Turb), total suspended solids (TSS), metal fractionation, was not done for all the events.

		Sampling information							Number of lab analyzes preformed							
Sampling point		Date	Rain [mm]	Antcendent dry period [min]	Rainfall duartion [min]	Sampling duration [min]	Total # samples	# samples paired	PSD	pH [a]	EC [a]	Turb [a]	TSS	Metal fractions		
														tot μm	1.2 μm	0.45 μm
HVS	U	25.02	SMLT[b]	-	-	455	21	21	21	21	21	21	21	21	21	21
	D					420	21		21	21	21	21	21	21	20	21
	U	06.03	25.1 [c]	680	950	75 [d]	4	3	4	3	3	3	3	2	2	2
	D					40 [d]	3		3	2	2	2	2	2	2	2
	U	20.03	SMLT[e]	-	-	370	19	13	18	18	18	18	19	13	13	13
	D					280 [d]	14		14	14	14	14	14	13	13	13
	U	22.03	16.4	1555	1085	15 [d]	1	1	-	-	-	-	1	-	-	-
	D					15 [d]	1		-	-	-	-	1	-	-	
	U	21.04	6.0	3635	925	20	1	1	1	1	1	1	1	1	1	1
	D					20	1		1	1	1	1	1	1	1	1
MSS	U	28.03	8.8	1020	360	630	8	8	8	-	-	-	-	-	-	-
	D					1110	20		20	-	-	-	-	-	-	-
	U	08.04	28.5	2340	360	1440	20	24	20	9	9	9	14	24	24	24
	D					1440	24		24	10	10	10	15	24	24	24
	U	20.04	3.8	14460	1500[f]	480	9	8	6	5	6	6	9	8	8	8
	D					480	22		22	11	13	14	22	8	8	8
	U	09.05	4.9	8640	240	180	10	10	10	9	9	9	10	9	8	8
	D					252	15		10	15	13	13	15	9	8	8

[a] pH, conductivity (EC) and turbidity (Turb) was analyzed according to the the standards ISO 10523:2008(ISO, 2008), NS-ISO 7888:1985 (ISO, 1985) and ISO 7027-1:2016 (ISO, 2016b), respectively.

[b] No precipitation recorded. Snow depth data from NCCS (2020), station SN68120 shows a decrease of 5 cm in the 24 hours before the sampling started. [c] Sludge/rain on snow [d] Sampling ended due to battery failing. [e] No precipitation recorded before the event started. Snow depth data from NCCS (2020), station SN68120 shows a decrease of 3 cm in the 24 hours before the sampling started. First precipitation registered after sampling finished. [f] A stay in precipitation of 5 hours within the period.

3.4 Sediment samples

To evaluate the treatment train upstream, the HVS samples of the sediments in the upstream gully pots were collected on the 5th of May 2021. Five gully pots were sampled as marked in Figure 1. All upstream gully pots could not be sampled due to safety reasons; see Appendix D. Before taking samples of the gully pots, the top water was abstracted by a vacuum vehicle. One grab composite sample of 1 liter was collected in plastic bottles from each gully pot using a Van Veen grab of stainless steel. The road was opened to traffic in November of 2018, and the sediment build-up was below 10 cm in the gully pots. Layering of sediments was therefore not an issue, as described by Adler (2020). All sediment samples were taken in the center of the gully pot. The Van Veen grab was first rinsed with water from the vacuum truck, followed by de-ionized water between sampling of each gully pot in order to prevent contamination. The samples were kept at 4°C until the lab analyses were performed.

3.4.1 Laboratory analysis

The PSD analyses of the sediment were performed based on the method developed by Adler (2020), utilizing manual wet sieving and a Beckman Coulter LS230 instrument. Manual weight-based wet sieving was used to sift particles between 50 and 2000 μm, giving a weight-based PSD. The sifted particles that came through a 50 μm sieve were diluted with distilled water and analyzed in the LS230 instrument, which yielded a number-based PSD.

Within short time particles in the highway runoff will form particle aggregates (Li et al., 2005). Therefore, a dispersant was used to disperse the agglomerations into their primary particles. The samples from each gully pot were split into two equal subsamples with a riffle splitter before they were analyzed in parallel; One with a natural appearance of the particles in the gully pot (NAT) and the second with added dispersant (DIS) using 3 g/L sodium pyrophosphate decahydrate ($Na_4P_2O_7$*$10H_2O$) in crystal form. The NAT sample was soaked overnight for at least 12 hours before the wet sieving began (NPRA, 1997).

Approximately 100 g of dry mass of each subsample was used for wet sieving to ensure sufficient mass for the largest sieves while preventing overloading of the smaller. This equated to approximately 300 g of wet sample (ISO, 2016a). Stainless steel sieves with a diameter of 200 mm and mesh sizes of 50, 75, 100, 150, 250, 1000, and 2000 μm placed over pre-weighed trays of stainless steel were used for sieving. The particles < 50 μm were collected in a tray underneath. The tray was mixed by hand before a sample was collected into a 100 mL plastic cup. To make sure that all particles were sieved, each sieve was flushed with approximately 0.5 L de-ionized water over a second tray. This water was then poured over the sieves with smaller mesh sizes before the flushing was repeated for the next sieve. The sieve tower was placed over a third tray before the same procedure of flushing was repeated. The particles left on the sieves were carefully transferred to pre-weighed beakers with distilled water. The beakers and trays with samples were dried at 105 °C into constant weight, according to the standard NS 4764 (Standards Norway, 1980), and weighed to determine the weight of each fraction. As in the method by Adler (2020), the particles above 2000 μm are not included to avoid underestimating smaller fractions.

The 100 mL plastic beaker containing a sample of the particles below 50 μm was gently mixed, and 10 mL was subtracted into a 50 mL plastic tube with a pipette. This was then diluted with distilled water up to 50 mL. The sample was analyzed in the LS230 as in Section 3.2.1 Laboratory analysis. For the DIS sample the dispersant (3 g/L $Na_4P_2O_7$*$10H_2O$) with distilled water was used as background liquid [2]. The organic matter in the sediment samples was determined according to NS 4764:1980 (Standards Norway, 1980) for the total and $<$50 μm fraction for each NAT sample.

2. The distilled water + 3 g/L $Na_4P_2O_7$*$10H_2O$ has a reflection index of 1.3335, which has to be set for the LS230. Distilled water has a standard reflection index for water at 1.3330

4 Results and discussion

This section examines the water quality parameters analyzed from the in - and outflow of the HVS and MSS. A discussion of pH, conductivity, and turbidity falls outside the main scope of this paper, but the parameters are included as a reference of the overall water quality. Secondly, the results of the sediment analyses will be presented to gain a better understanding of road runoff characteristics of the incoming water to the HVS. Lastly, the findings are discussed to describe design implications.

4.1 Particle removal efficiency

A majority of the particles bot at the HVS and MSS are smaller than 1 μm. Figure 2 represents the PSD of four runoff events at the HVS and two at the MSS. For the analyses of the MSS events on the 28th of March and 8th of April, the PIDS component was out of order, which resulted in no division of particles smaller than 0.4 μm. Findings show that over 90 % of the particles at the MSS were below 1 μm. At the HVS, 99 % of the particles were below 1 μm, with a median particle size of 0.134 $\pm$ 0.05 μm upstream and 0.152 $\pm$ 0.07 μm downstream. There is little difference in PSD in the inflow and outflow of the treatment facilities in most events in these results. However, as seen for event 6th of March (HVS) and 20th of April (MSS), some events show a shift in the peak towards larger particles in the outflow. This indicates the facility's ability to remove small particles less than 1 μm.

The two study sites differ in land use, AADT, climate, and geographic regions, which are factors that influence the composition of runoff (Kayhanian et al., 2012). Despite this difference, the inflow PSD to both the treatment facilities is smaller than expected. Smaller particles in the inflow of the HVS, however, might be caused by the complex upstream system with swales and several gully pots (Figure 1). A higher AADT might cause the particles to be swept further away, at the same time as they might crush into a smaller size due to the high traffic load.

Contrary to the findings of Strømberg (2020) and Westerlund and Viklander (2006) this study could not draw any clear differences between rain and snowmelt events due to limited data. However, in Figure 2 the curves on the snowmelt and rain/sludge on snow events the curves are more flattened than for the rain event 21st of April. This indicates smaller particles in road runoff during rain events. Neither this study nor the study by Strømberg (2020) have large enough data material to draw any conclusion, but based on the characterization of snowmelt, it is likely to assume bigger particles during snowmelt (Vijayan et al., 2019). PSD has been measured in road runoff in several studies (Westerlund and Viklander, 2006; Monrabal-Martinez et al., 2019; Selbig et al., 2016), but few of these are using a number based PSD over the range from 0.04 up to 2000 μm. A general method for determining PSD is still lacking. This make a comparison across studies challenging because there is none consistent experimental method. Westerlund and Viklander (2006) studied number-based PSD in the range 4 - 120 μm on a road with an AADT of 7400. The study reported that a range of 58 to 80 % of particles during rain and snowmelt events was in the smallest fraction between 4 - 6 μm. This emphasizes that smaller particles are largely represented both during snowmelt and rainfall. However, when comparing results to older studies, it must be pointed out that the particle range differs from this current study. Hence, the smallest particles are not included in the

statistics. The PSD in the current study skews towards smaller particles, with a majority of the particles well under 1 μm.

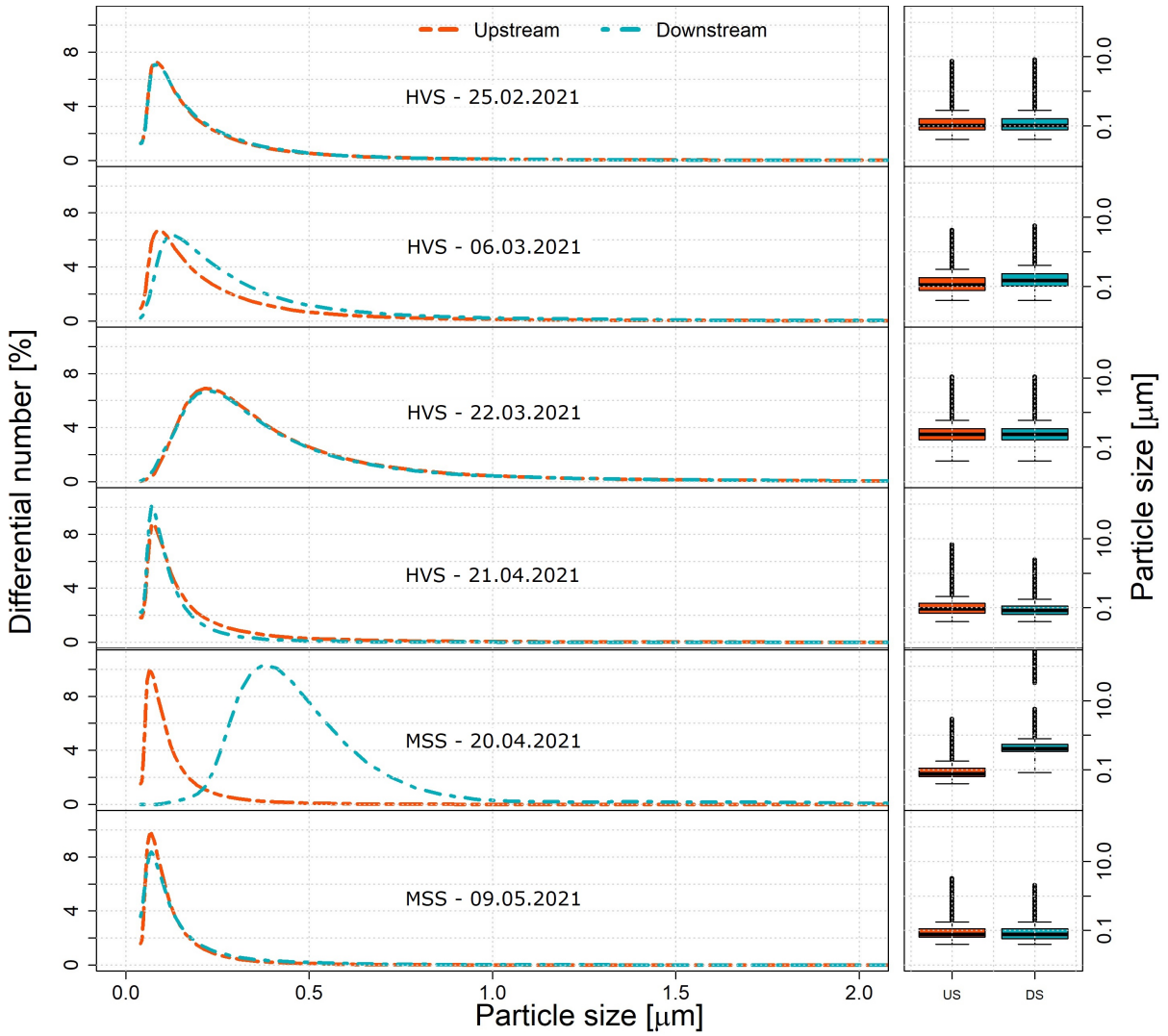

Figure 2: Particle size distribution of four events at the hydrodynamic vortex separator (HVS) and two of the events at the modular sedimentation system (MSS).

In order to further understand the inflow PSD, sediment samples were collected in the upstream manholes to investigate the PSD in these sediments. Wet sieving gave a mass-based PSD for the sediments in the upstream gully pots of the HVS, as represented in Figure 3. The fraction with particles below 50 μm is the largest for both NAT and DIS samples, with a median differential weight of 60 % for both. There is a minimal difference between the samples with and without dispersant, which Adler (2020) implies is due to weak bonds in the aggregation of particles. All the results from the sediments analyses are given in Appendix G. Strømberg (2020) analyzed the sediments in the HVS and the direct upstream gully pot, finding a contribution of 91 and 84 % in the < 50 μm fraction for the DIS and NAT samples, respectively. The smallest fraction increases in these gully pots, suggesting that coarser par-

ticles are removed in the upstream gully pots. However, all the gully pots at the study site have finer particles than sediments from gully pots in other Scandinavian cities with somewhat similar AADT, where the mass-based median particle ranged from 350 to 1500 μm (Karlsson and Viklander, 2008; Leikanger and Roseth, 2016).

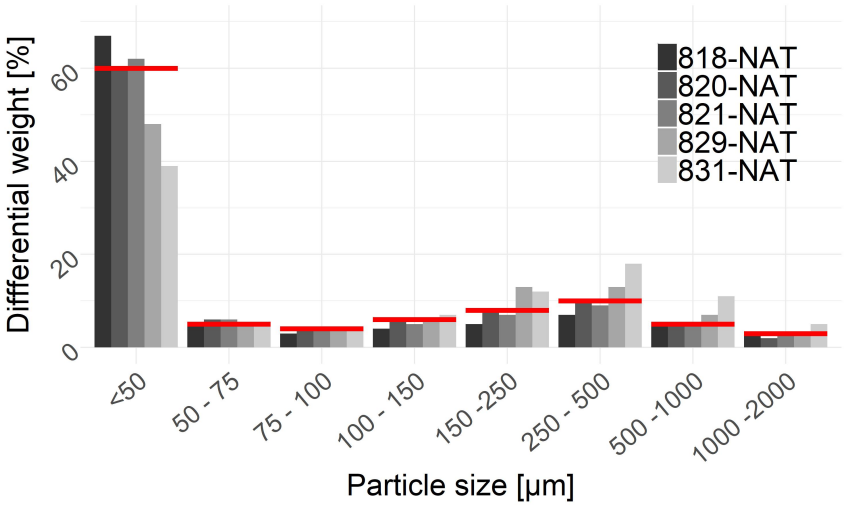

Figure 3: Particle size distribution of the sediment samples samples in the fractions without dispersant (NAT). The legend refers to the number of the gully pot, and the red line visualizes the median value within each fraction.

PSD analysis for the $<$ 50 μm fraction, which was done with a number-based approach, indicated that most of the particles are well below 1 μm. The median of the D_{90} are 0.204 μm and 0.234 μm for NAT and DIS samples, respectively. Together, the present findings, combined with Strømberg (2020), confirm that the road runoff at the site consists of small particles.

In the total fraction, organic matter ranged from 3.92 - 7.63 %. The organic part in the $<$ 50 μm fraction ranged from 7.23 - 11.3 %, with a median of 10 %. The findings are in line with the findings of Adler (2020), which showed that there is in general more organic matter in the fractons below 150 μm. Based on the smell and formation of a dark layer on top of the DIS-samples during drying, the organic part is most likely oil in the minuscule fraction. Leikanger and Roseth (2016) found a buildup of oil in gully pot sediments, which supports the implication of oil in the fraction $<$ 50 μm. Pictures from the analyses and of the dark film are found in Appendix G.

Total suspended solids (particles $>$ 0.45 μm) removal efficiencies at the HVS were observed in the range from 10 to 40 % during events with two or more paired TSS samples. The highest removal efficiency was found at the 25th of February event, while the event the 20th of March event had the lowest removal performance. Figure 4 represents TSS, pH, EC, and turbidity results of the paired samples from the two events together with boxplots that summarize the results of all paired samples at the HVS combined. Overall there is a reduction in TSS, EC, and turbidity for the HVS events combined. For each event, the TSS and turbidity show the same pattern. The pH remained between 7 and 8 in both the inflow and outflow at the HVS.

The 25th of February event produced the maximum peak of TSS concentrations recorded in the period in both the inflow and outflow with 813.8 mg/L and 745.1 mg/L. A reason for the high TSS concentration might be runoff generated by snowmelt, which is found to have higher contents of solids than rain-events (Westerlund et al., 2003; Helmreich et al., 2010). At the beginning of the event, TSS and turbidity are high before it stabilizes halfway through the event. This demonstrates activation of the swirl in the HVS, and particles are removed from the water phase. In the 20th of March event, a small removal efficiency is found as the TSS concentration in the inflow and outflow are following each other in a steady increase. A swirl in the HVS is probably not generated. Hence, the small removal is enhanced by standard sedimentation in the large water volume. It must be empathized that the inflow concentrations of TSS, EC, and turbidity are a tenfold larger in the first event than in the last event discussed. The low removal efficiency might somewhat be explained by this (Barrett, 2005; Strecker et al., 2001). The findings of varying and generally low removal efficiency ties well with previous studies of similar hydrodynamic separators done by Strømberg (2020) and Curwell (2015).

Both of the exemplified runoff events are generated by snowmelt. Therefore the developed SWMM model could not simulate the runoff at the HVS. However, from a weather station located 2 km away at the same altitude, the snow depth was recorded to decrease by 5 cm at the 25th of February and 3 cm on the 22nd of March. A higher flow, which started the swirl, may also explain the better removal efficiency at the first event. Curwell (2015) noted the importance of capturing the whole event when calculating the removal efficiency due to higher pollution concentrations at the beginning of an event. This is supported by the knowledge of higher toxicity and pollution in the first flush (Kayhanian et al., 2012; Li et al., 2008 and Cheng et al., 2017; among others). No discharge measurements were made during the sampling, but a depth of 3.5 cm and 3.0 cm in the inflow and outflow, respectively, was required for the sampling to start. A portion of the runoff was therefore passing before the pre-defined threshold value was reached.

Observations during sampling were done in the direct upstream and downstream manholes, showing that the pipes sometimes were dry. The recorded precipitation and diver data are presented in Appendix F. The diver data indicated a base flow that fluctuated around a depth of two centimeters. This was evaluated to be noise in the data, which was supported by the diameter of the diver of 18 mm. Consequently, the diver data was filtered resulting in that values under two centimeters were set to zero. The SWMM model was calibrated to a Nash–Sutcliffe model efficiency coefficient of 0.01, which means that the model has predictive skills slightly better than the mean of the observed data. This was acceptable for a simplified model, together with some uncertainties in the observed diver-data. The calibration yielded n-imperv to 0.39 and n-perv to 0.48. These are high manning values for asphalt and grass-covered swales compared to Manning's values given in the SWMM handbook table A.6 for overland flow and A.8 for channel-flow, which are 0.011 for asphalt and 0.03-0.4 for vegetated channels (Rossman, 2015). The high Manning's value slows the water down with the increased roughness, compensating for the swales and other unmodelled obstacles in the model upstream of the detention basin. The simulation of 30-year precipitation gave a maximum flow of 100 L/s at the HVS, with a 95 %-value of the total flow at 10 L/s. This value indicates the flow that reaches the HVS, but caution must be taken due to the uncertainties in the model and the fact that the precipitation data is from a weather station located 7 km northeast.

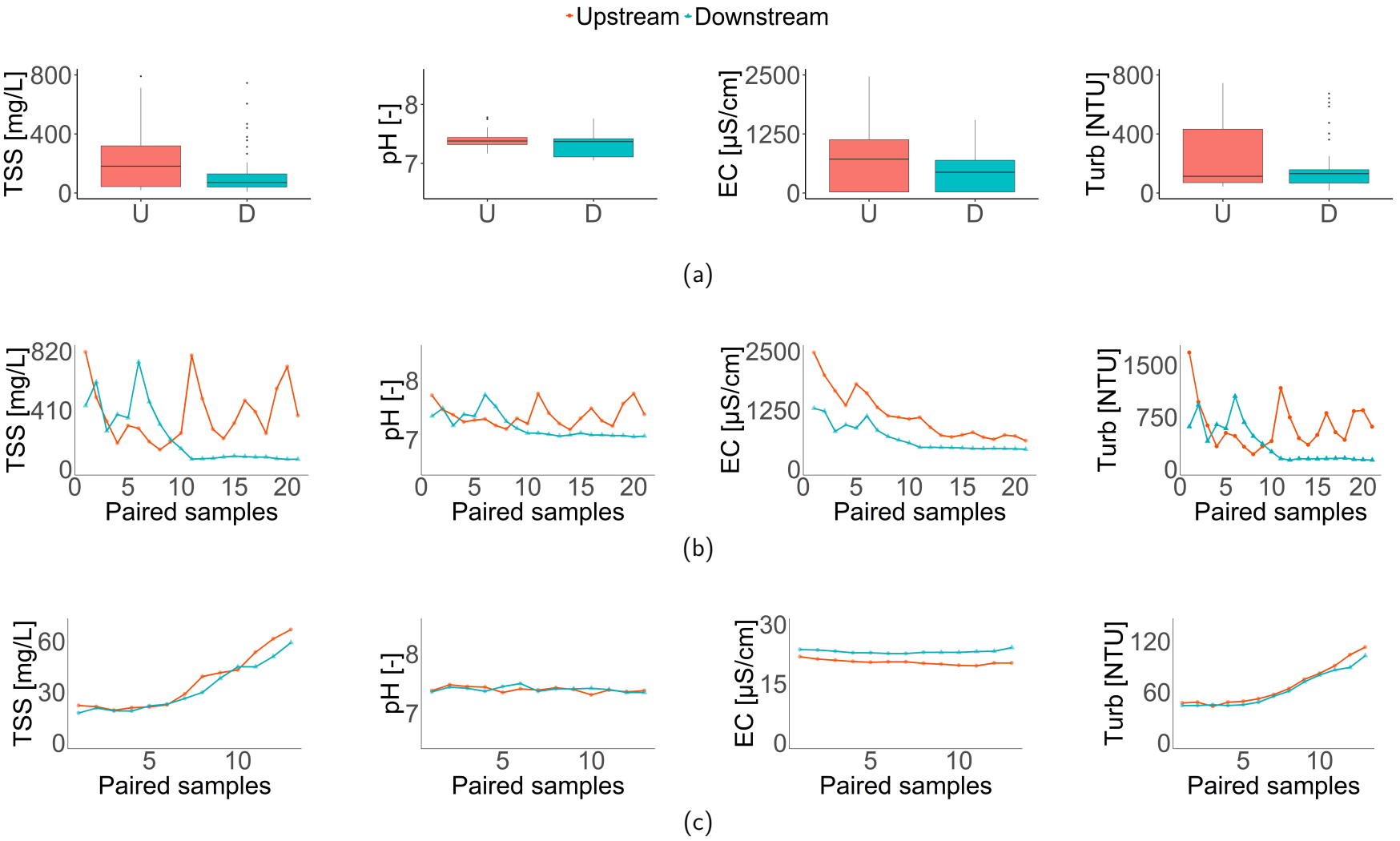

Figure 4: TSS, pH, electrical conductivity (EC) and turbidity from all paired samples at all sampled events (a), as well as the 25th of February (b) and 20th of March events at the HVS.

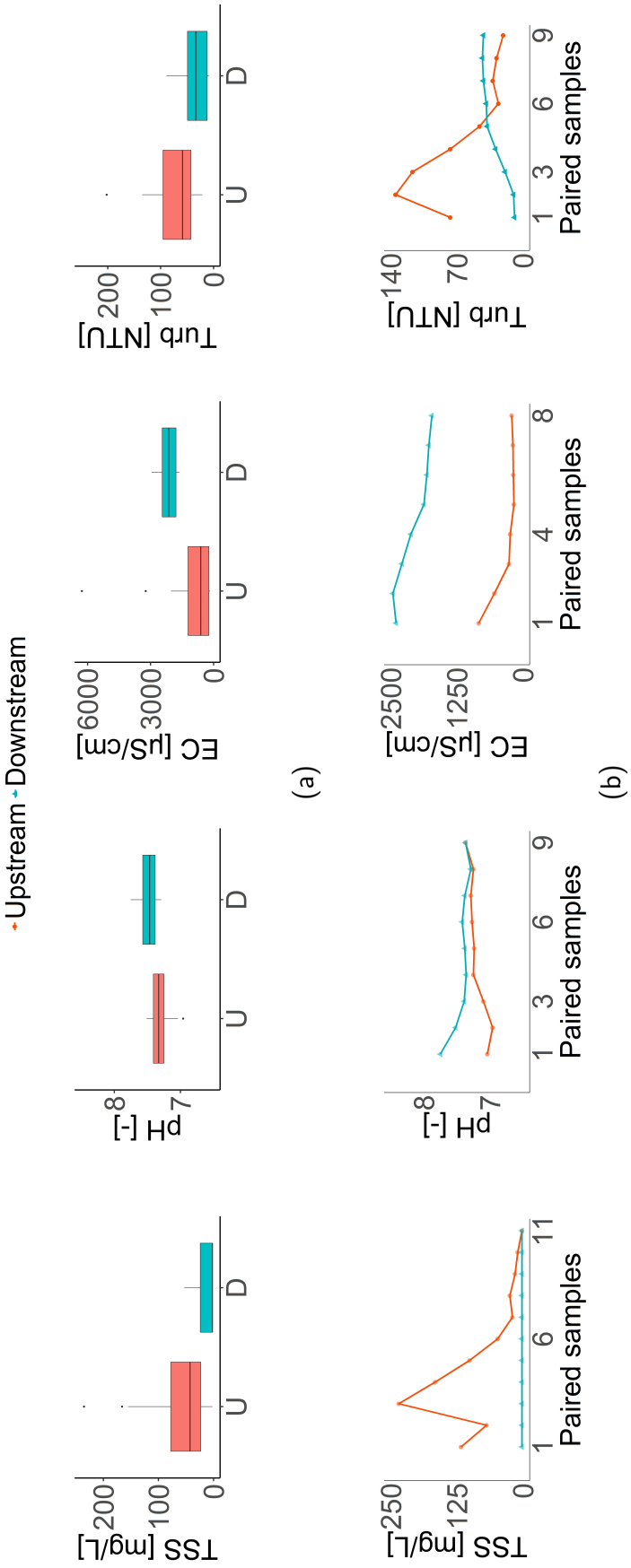

Figure 5: TSS, pH, electrical conductivity (EC) and turbidity from all paired samples at all events sampled at the MSS (a), followed by data from the 9th of May event (b). The downstream TSS consentration is below the report limit at 2 mg/L.

The removal efficiency at the MSS of total suspended solids was recorded to be 48 %, 92 % and 98 % for the events 8th and 20th of April and 9th of May event, respectively. The highest precipitation was recorded on the first event, which likely also generated the highest flow into the MSS. As the incoming volume is larger, the time for settling will decrease. With a low settling velocity, small particles such as those found at the MSS will not have enough time to settle (Li et al., 2008). At the same time, larger runoff intensities might bring larger particles to the treatment facility that will according, to Stoke's law, sedimentate faster. Figure 5 represents results of TSS, pH, EC and turbidity analyzes for all paired samples summarized and for the 9th of May event. The reduction of TSS and turbidity follow the same pattern, with a clear reduction totally from the inflow to the outflow. Li et al. (2006) suggests that these two parameters can be useful surrogates for each other, as they show a strong correlation. At the exemplified event 9th of May, the turbidity rises over the inflow halfway through the event. Explanations for this might be that some of the water in the outflow had a long residence time or that some particles were re-mobilized. An interesting finding is that both pH and EC rise from the inflow to the outflow. This supports the hypothesis of re-suspension of some particles in either the sedimentation chambers or in the downstream manhole.

Paired samples for four out of five events at the HVS and three out of four events at the MSS were analyzed for Ni, Cu, Zn, Cd, and Pb. The total in-and outflow concentrations for the Ni, Cu, Zn, and Pb are given in Figure 6. The Cd concentration is given for the dissolved fraction in both plots due to methodological limitations. All metals, except for Cd where data is not available, are found to be present in both the particulate and dissolve forms. This is in line with findings from Kayhanian et al. (2012). The events earlier discussed are shown in Figure 7, 8, and 9 to show how the metal concentrations develop over time in the inflow and outflow. The annual average environmental quality standard (AA-EQS) values for Cu (7.8 μg/L) and Zn (11 μg/L) are found in the guide for classification of water by Norwegian Environment Agency (2016), while for values for Ni (4 μg/L), Cd (0.08 μg/L [3]), and Pb (1.2 μg/L) are also found in the Water Regulation (Vannforskriften, 2006). Long-term exposure in the recipient of concentrations greater or equal to the AA-EQS value will cause chronic effects. Acute toxic effects may occur if the metal concentrations are above the acute predicted no effect concentration, PNEC$_{acute}$ (Norwegian Environment Agency, 2016). According to Appendix VIII E in the Water Regulation (Vannforskriften, 2006) the EQS values for Cu and Zn given for the total concentration in the water sample, while for Ni, Cd, and Pb, the values are current for the dissolved concentrations ($<$ 45 μm), which are the most bio-available. Notwithstanding, total metal concentrations for Ni and Pb are presented as an overview for all samples because both the facilities investigated are intended to remove particles.

Total Cadmium was under the detection limit of the ICP-MS for all samples. The same occurred for Ni at the HVS's 20th of March event and the MSS's 8th of April event. This uncovers some weaknesses of the method since the 1.2 μm, and 0.45 μm filtrate was detected. The most significant error in the method is probably the dilution of the total samples after UltraClave digestion. A dilution must be done to transfer the samples from the silicone tubes used during UltraClave to metal-free tubes. However, an option is to provide more sample

3. Minimum value. The limit depends of the hardness of the water (Vannforskriften, 2006).

volume into the UltraClave to reduce the effect of dilution. Another weakness is the overlap of fractions for some metals, especially for Ni and Cd, as seen in Figure 7, 8, and 9. The overlap should by theory not occur but might be caused by several errors, for example, sample contamination. In the event 20th of March, Figure 8, there might be a switch between the samples, as the peaks in the total and 1.2 μm filtrate are offset from each other.

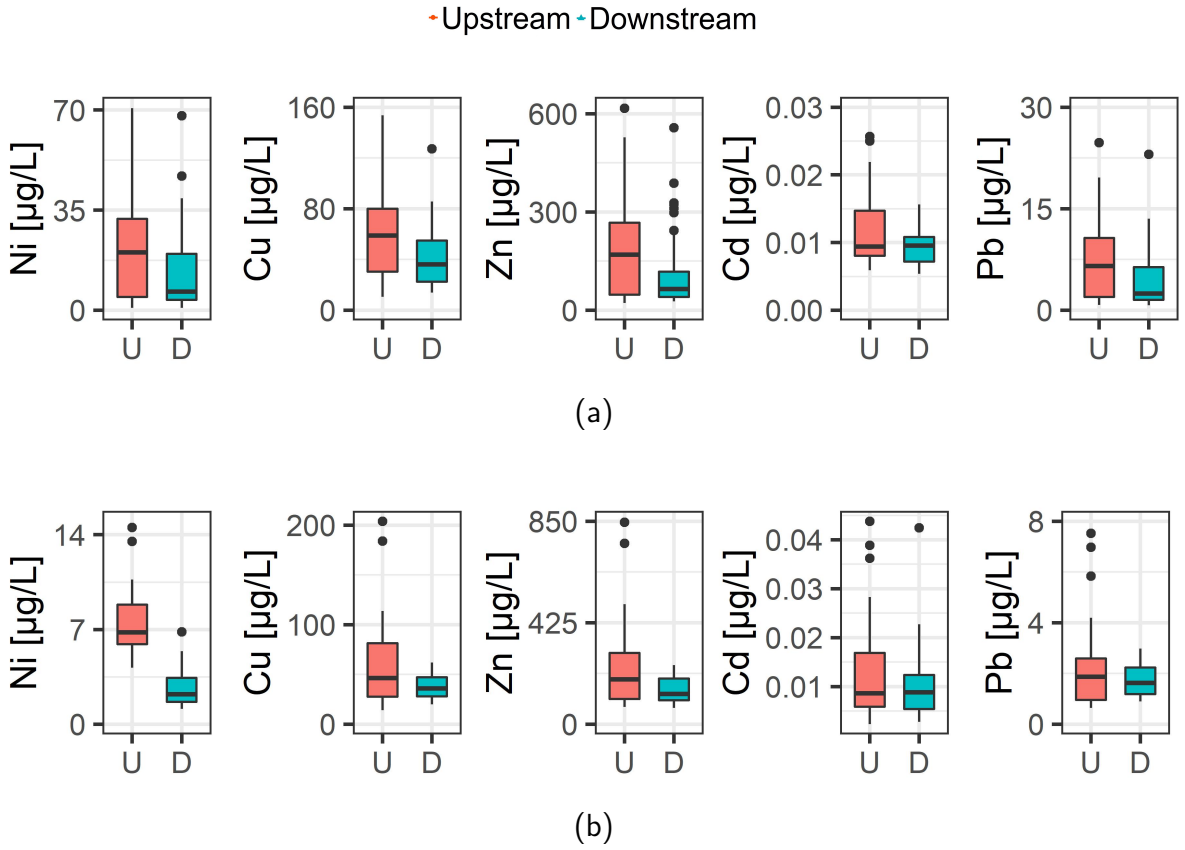

Figure 6: Representation of all in -and outflow concentrations of Ni, Cu, Zn, Cd, and Pb for all the paired samples from the HVS (a) and MSS (b). The total concentrations are represented for all the metals except for Cd, where the dissolved concentration is shown due to invalid results for the total. For some samples at the 20th of March event, Ni results were reported under the detection limit.

In the monitored events at the HVS and MSS, the average dissolved concentration for Ni, Cd, and Pb never exceeds the AA-EQS, while Cu and Zn have exceeded the threshold both the inflow and outflow. If Ni, Cd, and Pb concentrations were too high, the HVS and MSS would initially not have been a good choice of treatment solution since they aim to remove particulate matter. At the HVS, the metals of concern, Cu and Zn, had on average 83 and 94 % of the concentrations in the particulate fraction at the inflow and outflow, respectively. The average concentration in the outflow was nearly three times the value of $PNEC_{acute}$ = 15.6 μg/L for Cu and two times the value of the $PNEC_{acute}$ = 60 μg/L for Zn. Average outflow concentrations of Cu and Zn at the MSS were both 2.4 times larger than the respective $PNEC_{acute}$ threshold value. The dissolved fraction in the inflow constituted 60 % of the total

Cu concentration, while in the outflow, this shifted to only 40 %. For Zn, the concentration of Zn in the particulate grew from 28 to 40 %. This increase of concentration in the particulate fraction was unexpected because one would think that the particles settle. Nevertheless, the same trend is found in the PSD for the 20th of April event, where the particles are skewed towards larger particles in the outflow. At the same time, it might also explain the increased EC in the outflow of the MSS.

Values above $PNEC_{acute}$ in the outflow are not necessarily a threat to the downstream recipient, but further investigations should be done of the recipient to make sure concentrations are not surpassing. The typical low volume from the treatment device in proportion to the recipient often dilutes the concentrations sufficiently. However, high concentrations above $PNEC_{acute}$ in the outflow should be checked with caution, as these can threaten the aquatic environment.

A larger variation in concentration is found in the inflow for each of the metals than in the outflow. The highest concentrations of metals, as well as TSS, occurred during the 25th of February event at the HVS, which was caused by significant snowmelt. All paired metal concentrations for the event are presented in Figure 7. For Ni, Cu, Zn, and Pb the same trend as for TSS (Figure 4, (b)) can be seen, with a clear reduction in concentration in the middle of the event. This demonstrates that the HVS has the ability to remove metals when the swirl starts. Despite a higher AADT at the highway draining to the HVS, the metal concentration are solely not more significant than at the MSS. Recorded inflow concentrations of Ni and Pb are highest at the HVS, while Cu, Zn, and Cd are larger at the MSS. The differences might be caused by differences in land use, AADT catchment size, geographic region, total event rainfall, and antecedent dry period, which Kayhanian et al. (2012) reports to significant influence pollutant concentrations.

Statistical analyses was not performed in this study, but previous studies have investigated the correlation between TSS, PSD, and metal concentrations in road runoff (Ferreira et al., 2013; Meland, 2018; Westerlund and Viklander, 2006; Sansalone et al., 1995; among others). Sansalone et al. (1995) found a strong correlation between the heavy metals investigated in the current study and TSS at E6 further south of the HVS study site, in Jessheim. The correlation was strongest for small particles < 15 μm and during snowmelt events. This was expected as smaller particles have an increased specific surface area (Sansalone et al., 1995) and more available material containing heavy metals to adsorb to the particles (Westerlund and Viklander, 2006). Meland (2018) studied untreated tunnel wash water, which can be characterized as a hot spot within road runoff due to the high pollution concentrations. The study demonstrated a correlation ranging from 0.86 to 0.90 between TSS and the metals Ni, Cu, Zn, and Pb. As a result of this, Meland (2018) suggests that TSS can be used to estimate other pollution concentrations. Contrary to the findings of the discussed studies Ferreira et al. (2013) did not find a strong correlation with TSS and the particulate-phase metal concentration. Removal of TSS and heavy metals do not seem to have a strong relationship at the MSS either, as the removal efficiency of TSS at the 9th of May event was 98 %, while for the metals it is ranging between 42 and 55 % (see Appendix E, Removal efficiencies). In Figure 9, which represents the evolution of metals in the inflow and outflow of the event, it can also be seen that metal concentrations in the outflow are above the AA-EQS value.

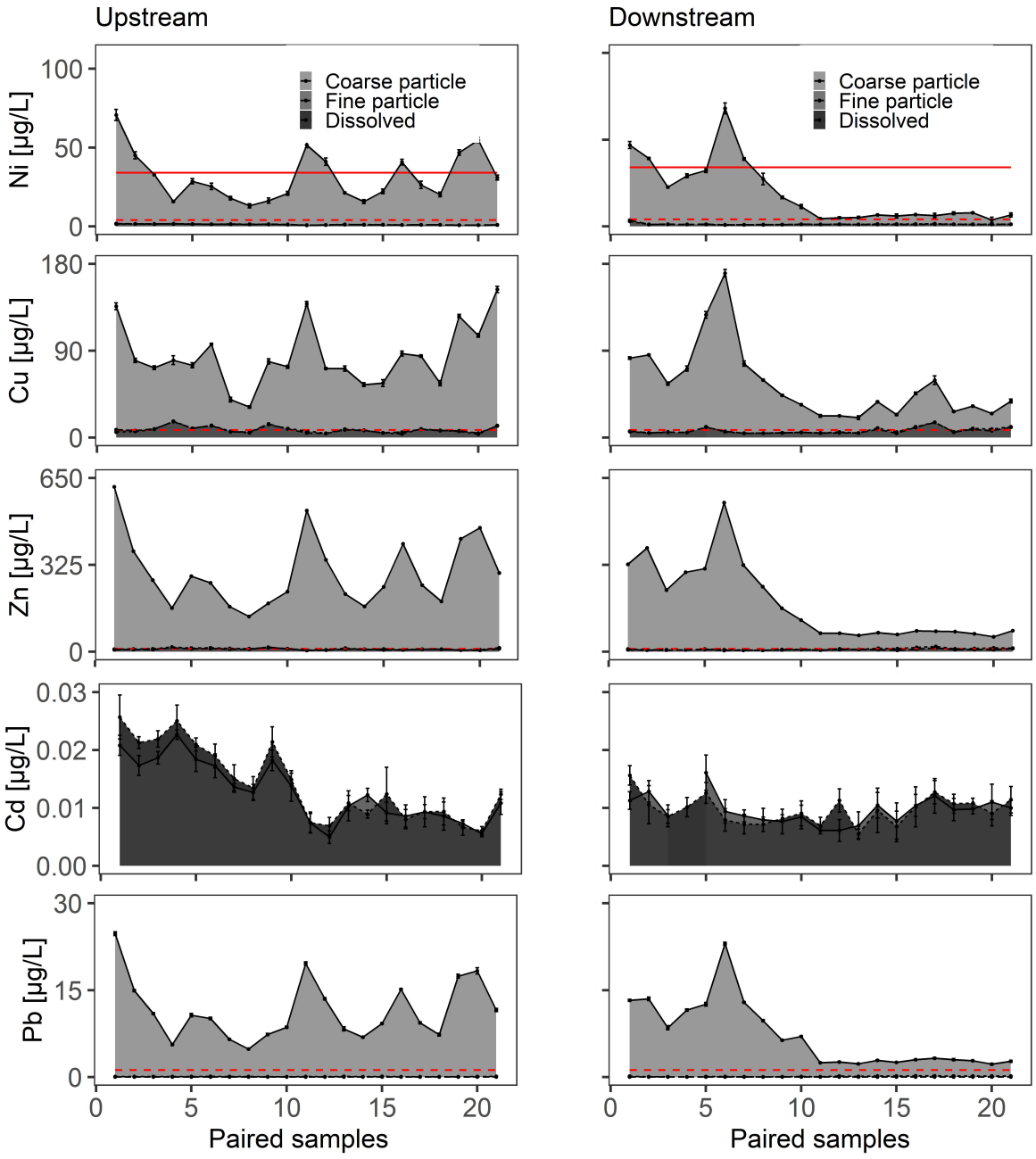

Figure 7: Metal concentrations of Ni, Cu, Zn, Cd, and Pb from the 25th of February event at the HVS. The upstream and downstream concentrations are represented to the left and right, respectively. For each sample, the error bar represents the relative standard deviation. AA-EQS values for the individual metal in freshwater are shown with the red dashed line. For Ni, Cd, and Pb, the AA-EQS values are current for the dissolved fraction.

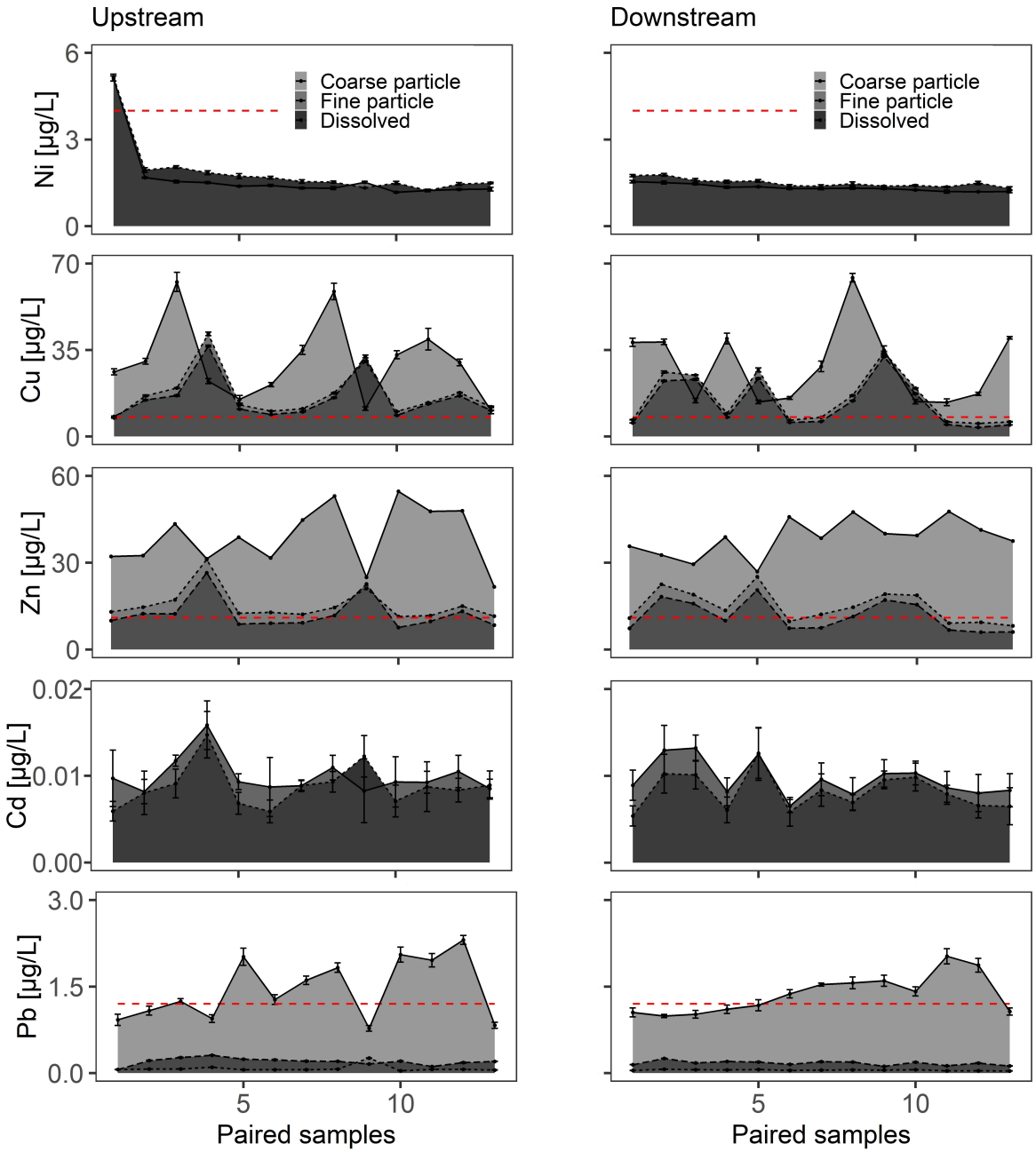

Figure 8: Metal concentrations of Ni, Cu, Zn, Cd, and Pb from the 20th of March event at the HVS. The upstream and downstream concentrations are represented to the left and right, respectively. For each sample, the error bar represents the relative standard deviation. AA-EQS values for the individual metal in freshwater are shown with the red dashed line. For Ni, Cd, and Pb, the AA-EQS values are current for the dissolved fraction. Ni is represented without a coarse particle fraction due to concentrations under the detection limit.

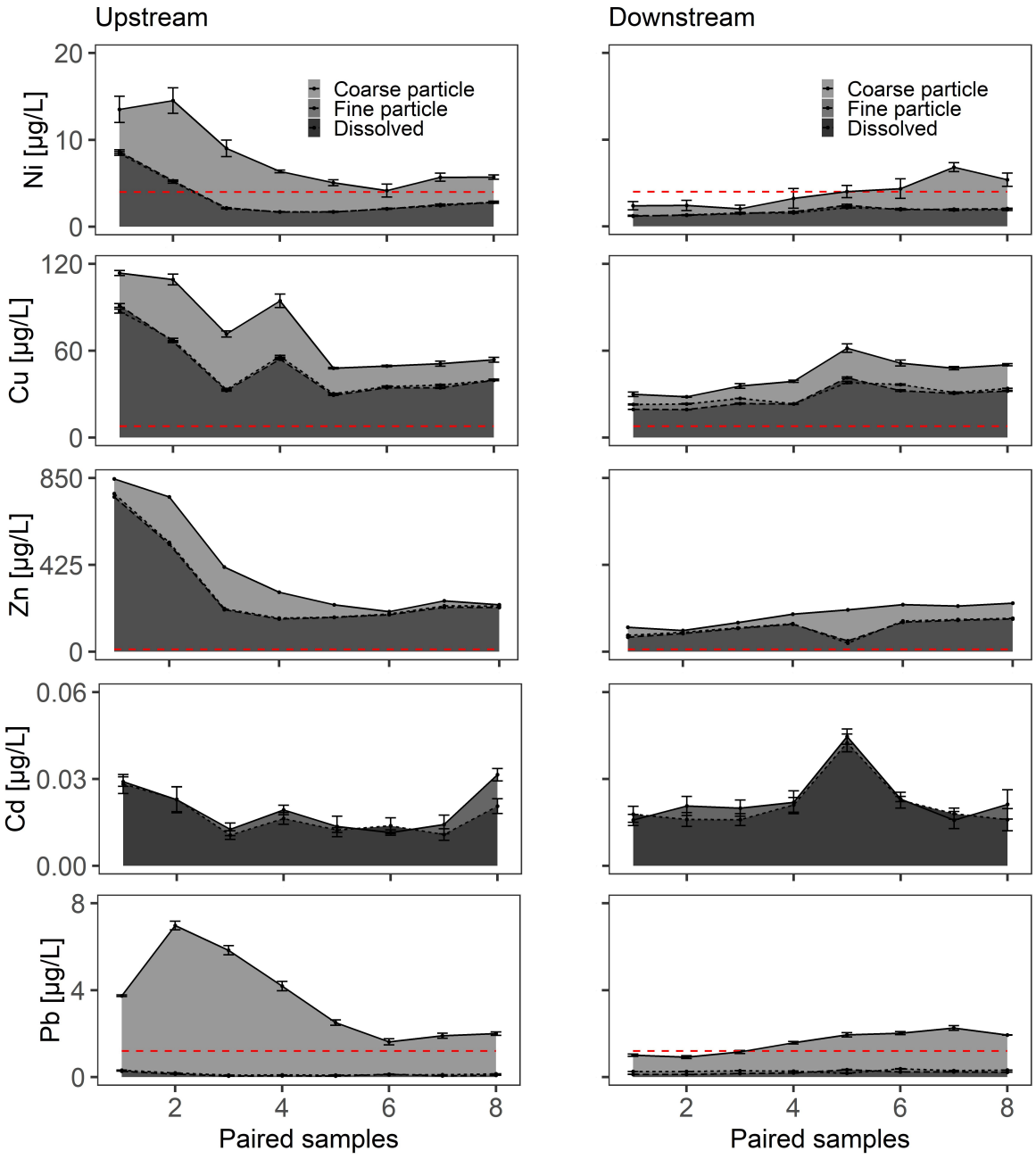

Figure 9: Metal concentrations of Ni, Cu, Zn, Cd, and Pb from the 9th of May event at the MSS. The upstream and downstream concentrations are represented to the left and right, respectively. For each sample, the error bar represents the relative standard deviation. AA-EQS values for the individual metal in freshwater are shown with the red dashed line. For Ni, Cd, and Pb, the AA-EQS values are current for the dissolved fraction.

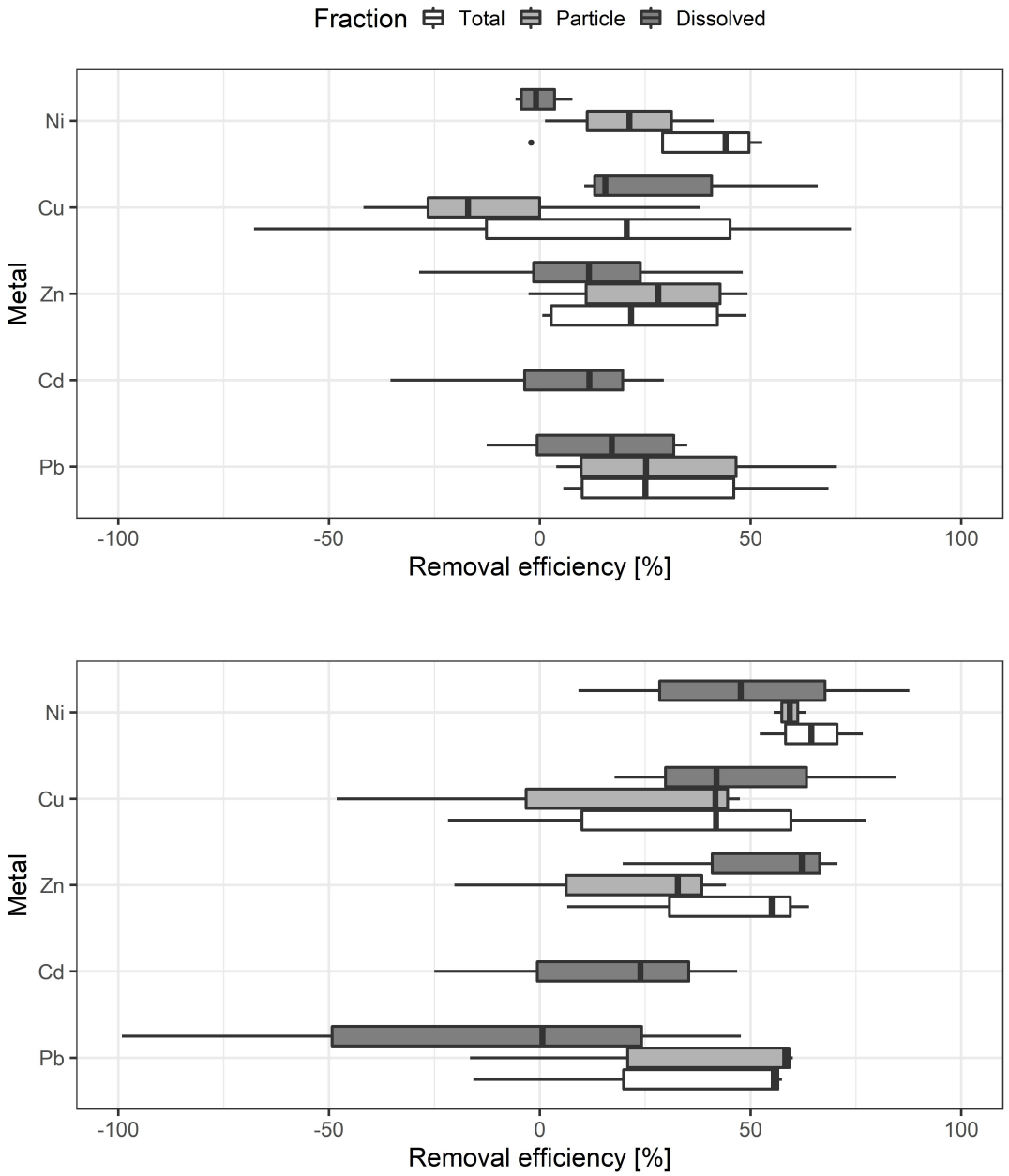

Figure 10: The removal efficiency of each event for metals in the total, particle, and dissolved fractions for the hydrodynamic vortex separator (top) and modular sedimentation system (bottom). The particulate Nickle concentration of 22nd of March and 21st of April event at the HVS and the 8th of April event at the MSS were not included due to a negative particulate fraction value. Cadmium is exclusively presented in the dissolved fraction.

The removal efficiency varies between the metals and the events at both the HVS and MSS, shown in Figure 10. All over, Ni had the highest removal efficiency, where most of the removal is found in the particulate fraction. The total median removal efficiency is above zero for all metals, but it is negative for Cu and Pb for some events. However, Cu and Zn are the only metals that are above the AA-EQS value in the outflow.

4.2 Implications for step one water quality treatment measures

From the modeling and water quality parameter results, it is clear that the HVS and the upstream treatment train have an improper design. The supplier of the HVS in this current study reports retention of 80 % for events with flows of 192 L/s and particles $\geq$ 110 μm. However, a flow regulator restricts the discharge entering the HVS to 135 L/s. Therefore, it will not be possible to reach optimal flow conditions in the HVS. Results from flow modeling in SWMM imply that over a 30-year period, the flow of 192 L/s would not have been reached even without the flow regulator. An extensive treatment measure is here direct against its intention because the everyday events have a low treatment efficiency. A suggested better position of the HVS would be upstream of the detention basin, as shown in Appendix A; Figure A3, to ensure more significant flows entering the treatment facility. Hence, the swirl could start in more events, and an all-over better treatment efficiency could be obtained. The same results could possibly be gained by reducing the size of the HVS, which would also have reduced the initial installation costs. A smaller device would require more frequent sediment removal from the storage, but this could give benefits in the form of hindering the sedimented pollutants in re-mobilization. Even though the flow was greater than the optimal treatment flow, the HVS has a large hydraulic capacity. The studied HVS have a maximum capacity of 540 L/s (Miljø- og Fluidteknikk AS, 2020).

The findings of that 99 % of the particles are smaller than 1 μm raises concern if a HVS is a suitable treatment device at the site. Large numbers of small particles at the HVS can contribute to findings of low treatment efficiencies of TSS at the HVS. From the supplier, the 80 % retention is given for particles $\geq$ 110 μm, which is not present at this site. Laboratory testing, of the same HVS as investigated in this study, performed by NJCAT Technology Verification (2015) gave TSS removal efficiency of 55 %, but this was without particles smaller than 1 μm. TSS analyses in the current study only measure particles over 0.45 μm, while 90 % of the particles found in the inflow were below 0.316 $\pm$ 0.11 μm. Even though most particles are small, they may contribute little to the total mass (Li et al., 2005). However, due to the high specific surface area, these very small particles can carry harmful pollutants such as heavy metals and polycyclic aromatic hydrocarbons (PAH) (Sansalone and Buchberger, 1997a). The fine particles are of great concerns as they can cover spawning ground for fish and disturb aquatic biota at even low concentrations (Nøst, 2019; Meland, 2010). The investigated particle removal systems aim to remove particles, but the fine matter is proven to be of concern. Analyses of the sediments in the upstream gully pots of the HVS substantiate that the road runoff contains in large parts small particles.

In the sampling period, no storms were generating volumes close to the design size of the treatment devices. Contrary to the HVS, small inflow volumes at the MSS can improve treatment efficiency due to longer residence time. However, both Li et al. (2008) and Cheng et al. (2017), underlines that capturing of the first flush in design storms will constitute a considerable particle removal effect, due to detention of the most polluted runoff. With a capturing of 35 % of the total runoff volume, the latter study found a removal of 74 % of the total TSS ($>$ 1.5 μm). The MSS has a large hydraulic capacity, and TSS removal results suggest that the efficiency is good for everyday events. At the same time, the removal of metals, especially Cu and Zn, might not be sufficient. A larger treatment compartment will

probably not be the preferred solution to remove these metals, but rather a solution to remove dissolved matter. This is because a large fraction of the remaining Cu and Zn are in the dissolved phase. For the HVS, on the other hand, a more optimal particle removal solution will be adequate.

The MSS is designed for a storm with at least a 20 year return period (Storm Aqua AS, 2021). Such a large design would not be necessary to treat everyday events. However, the sedimentation system also serves as a detention basin. Hence, the MSS is a combined step one and step two measure according to the three-step approach. For traditional sedimentation devices, such as sedimentation tanks and basins, a design that combines the intent of step one and two might be a good implementation, as this enhances particle removal by increasing the residence time with larger dimensions (Li et al., 2008).

This study points to that step one road runoff quality measures with advantage for all over treatment efficiency, costs, and maintenance for certain treatment solutions. Cheng et al. (2017) and Kayhanian et al. (2008), among others, implied the importance and large effect of treating the first flush in runoff events. By designing step one treatment measures to treat 95 % of the yearly precipitation, the capacity for treating the first flush will also always be available. A bypass should convey water past the treatment measure when the maximum capacity of the device is reached. For devices like hydrodynamic vortex separators, where certain flows are necessary to obtain the desired treatment efficiency, smaller treatment compartments will cause these flows to more frequently be reached. The area requirements and costs of the treatment measurements will decrease (Paus, 2018), which will make treatment solutions easier to prioritize and include in more projects (Ranneklev et al., 2016).

5 Conclusion

The removal efficiencies of total suspended solids (TSS) in this study ranged from 10 to 40 % at the hydrodynamic vortex separator (HVS), while a higher performance was obtained by the modular sedimentation system (MSS) varying from 48 to 98 %. Metal removal efficiencies varied between site, metals, and fractions, but Cu and Zn were the only metals that surpassed the environmental quality standards in the outlet. At both sites, over 90 % of the particles were below 1 μm, with a particle size distribution (PSD) skewed towards the smallest particles at the HVS. Sediments in a number of the gully pots upstream the HVS were investigated, revealing that also these consisted of a majority of small particles. The high number of small particles was unexpected, as the investigated treatment solutions aim to remove particles by sedimentation. At the HVS, the highest removal efficiency occurred at high flows, such that the swirl inside the HVS started and enhanced the particle removal. Contrary, at the MSS, the lowest removal efficiency was found during the event with the most precipitation. An explanation is that the residence time for the particles was lower. Consequently, the small particles did not have time to sedimentate. The study has demonstrated the importance of investigating the PSD and the pollutants of interest before design.

Findings from the study of the HVS imply that several of step one solutions can be designed smaller, for example, to treat 95 % of the yearly precipitation volume. With such a design approach, some water in larger storms will be bypassed, but the everyday events and the first flush will be treated. For devices like the HVS, the results indicate that large treatment solutions reduce treatment efficiency because optimal conditions infrequent occur. Smaller devices will presumably result in better removal efficiencies, as well as require less area and costs. In cases where it is favorable that step one, treatment, and step two, detention, are combined, large treatment solutions like the MSS can be adequate. In everyday events, the MSS has a large capacity. Hence, it is a long hydraulic residence time that is favorable for particle removal. The number of events monitored in this study is limited; therefore, more events should be studied to conclude.

Further investigations of the MSS will help to gain a better understanding of how combined step one and step two solutions work. An investigation of the recipient downstream of the MSS is also proposed, as the Cu and Zn concentrations may harm the aquatic environment. Regarding the design of the HVS, further studies of smaller devices, road runoff with small particles, and differences in removal efficiency of standard gully pots compared with HVSs are suggested to learn their optimal use. Lastly, this work can hopefully be used as a base for developing a set of design criteria for the design of step one treatment solutions.

6 References

Adler, Nadine. 2020. "Performance of Road Side Gully Pots in Trondheim for Sediment Removal." Master's thesis, Norwegian University of Science and Technology. https://hdl.handle.net/11250/2656744.

Aldheimer, G., and K. Bennerstedt. 2003. "Facilities for Treatment of Stormwater Runoff from Highways." *Water Science and Technology* 48 (9): 113–121. https://doi.org/10.2166/wst.2003.0505.

Andoh, R.Y.G., and A.J. Saul. 2003. "The Use of Hydrodynamic Vortex Separators and Screening Systems to Improve Water Quality." *Water Science and Technology* 47 (4): 175–183. https://doi.org/10.2166/wst.2003.0248.

Ball, J E, R Jenksb, and D Aubourgb. 1998. "An Assessment of the Availability of Pollutant Constituents on Road Surfaces." *The Science of the Total Environment,* 12.

Barrett, Michael E. 2005. "Performance Comparison of Structural Stormwater Best Management Practices." *Water Environment Research* 77 (1): 78–86. https://doi.org/10.2175/106143005X41654.

Beck, Hylke E., Niklaus E. Zimmermann, Tim R. McVicar, Noemi Vergopolan, Alexis Berg, and Eric F. Wood. 2018. "Present and Future Köppen-Geiger Climate Classification Maps at 1-Km Resolution." *Scientific Data* 5 (1): 180214. https://doi.org/10.1038/sdata.2018.214.

Beckman Coulter. 2011. *Coulter LS Series Product Manual.* https://www.beckmancoulter.com/wsrportal/techdocs?docname=4237214EA.pdf.

Butler, D., and S. H. P. G. Karunaratne. 1995. "The Suspended Solids Trap Efficiency of the Roadside Gully Pot." *Water Research* 29 (2): 719–729. https://doi.org/10.1016/0043-1354(94)00149-2.

Cheng, Jing, Qingke Yuan, and Kim Youngchul. 2017. "Evaluation of a First-Flush Capture and Detention Tank Receiving Runoff from an Asphalt-Paved Road." *Water and Environment Journal* 31 (3): 410–417. https://doi.org/10.1111/wej.12258.

Curwell, Thomas. 2015. "An investigation into the quantification and mitigation of urban diffuse pollution." PhD diss., University of Salford. http://usir.salford.ac.uk/id/eprint/36223.

Direktoratsgruppen vanndiriktivet. 2018. *Veileder 02:2018 Klassifisering Av Miljøtilstand i Vann.* https://www.vannportalen.no/veiledere/klassifiseringsveileder/.

EPA, United States Environmental Protection Agency. 2020. *Storm Water Management Model (SWMM). Version 5.1.015.* https://www.epa.gov/water-research/storm-water-management-model-swmm.

Fardel, Alexandre, Alexandre Fardel, Pierre-Emmanuel Peyneau, Pierre-Emmanuel Peyneau, Béatrice Béchet, Béatrice Béchet, Abdelkader Lakel, Abdelkader Lakel, Fabrice Rodriguez, and Fabrice Rodriguez. 2019. "Correction to: Analysis of swale factors implicated in pollutant removal efficiency using a swale database." *Environmental science and pollution research international* (Berlin/Heidelberg) 26 (2): 1303–1303. https://doi.org/10.1007/s11356-018-3846-5.

Ferreira, M., S.-L. Lau, and M. K. Stenstrom. 2013. "Size Fractionation of Metals Present in Highway Runoff: Beyond the Six Commonly Reported Species." *Water Environment Research* 85 (9): 793–805. https://doi.org/10.2175/106143013X13736496908870.

Helmreich, Brigitte, Rita Hilliges, Alexander Schriewer, and Harald Horn. 2010. "Runoff Pollutants of a Highly Trafficked Urban Road – Correlation Analysis and Seasonal Influences." *Chemosphere* 80 (9): 991–997. https://doi.org/10.1016/j.chemosphere.2010.05.037.

Hoffman, Eva J., James S. Latimer, Carlton D. Hunt, Garry L. Mills, and James G. Quinn. 1985. "Stormwater Runoff from Highways." *Water, Air, and Soil Pollution* 25 (4). https://doi.org/10.1007/BF00283788.

Huerta-Diaz, Miguel Angel, Ignacio Rivera-Duarte, Sergio A. Sañudo-Wilhelmy, and A. Russell Flegal. 2007. "Comparative Distributions of Size Fractionated Metals in Pore Waters Sampled by in Situ Dialysis and Whole-Core Sediment Squeezing: Implications for Diffusive Flux Calculations." *Applied Geochemistry* 22 (11): 2509–2525. https://doi.org/10.1016/j.apgeochem.2007.07.001.

ISO, International Organization for Standardization. 2016a. *Geotechnical investigation and testing - Laboratory testing of soil - Part 4: Determination of particle size distribution [ISO 17892-4].* https://www.standard.no/no/Nettbutikk/produktkatalogen/Produktpresentasjon/?ProductID=877569.

———. 1985. *Water Quality - Determination of Electrical Conductivity [ISO 7888].* https://www.standard.no/no/Nettbutikk/produktkatalogen/Produktpresentasjon/?ProductID=146721.

———. 2008. *Water Quality - Determination of pH [ISO 10523].* https://www.standard.no/no/Nettbutikk/produktkatalogen/Produktpresentasjon/?ProductID=529464.

———. 2016b. *Water Quality - Determination of Turbidity - Part 1: Quantitative Methods [ISO 7027-1].* https://www.standard.no/no/Nettbutikk/produktkatalogen/Produktpresentasjon/?ProductID=832960.

Karlsson, Kristin, and Maria Viklander. 2008. "Trace Metal Composition in Water and Sediment from Catch Basins." *Journal of Environmental Engineering* 134 (10): 870–878. https://doi.org/10.1061/(ASCE)0733-9372(2008)134:10(870).

Kartverket. 2021. *Topografisk Norgeskart 4 [WMS]. Scale 1:500 til 1:10M.* https://openwms.statkart.no/skwms1/wms.topo4.

Kayhanian, Masoud, Boaz D. Fruchtman, John S. Gulliver, Comasia Montanaro, Ezio Ranieri, and Stefan Wuertz. 2012. "Review of Highway Runoff Characteristics: Comparative Analysis and Universal Implications" [in en]. *Water Research,* Special Issue on Stormwater in Urban Areas, 46, no. 20 (December): 6609–6624. ISSN: 0043-1354. https://doi.org/10.1016/j.watres.2012.07.026.

Kayhanian, Masoud, Chris Stransky, Steven M. Bay, Sim-Lin Lau, and Michael K. Stenstrom. 2008. "Toxicity of Urban Highway Runoff with Respect to Storm Duration." *Science of The Total Environment* 389 (2): 386–406. ISSN: 0048-9697. https://doi.org/10.1016/j.scitotenv.2007.08.052.

Kim, Jong-Yeop, and John J. Sansalone. 2008. "Event-Based Size Distributions of Particulate Matter Transported during Urban Rainfall-Runoff Events." *Water Research* 42 (10): 2756–2768. https://doi.org/10.1016/j.watres.2008.02.005.

Lee, D. H., K. S. Min, and J.-H. Kang. 2014. "Performance Evaluation and a Sizing Method for Hydrodynamic Separators Treating Urban Stormwater Runoff." *Water Science and Technology* 69 (10): 2122–2131. https://doi.org/10.2166/wst.2014.125.

Leikanger, Eirik, and Roger Roseth. 2016. *Veiavrenning og driftstiltak. Overvåking av avrenning samt oppfølging av feie- og sandfangmasser ved ulik veidrift.* NIBIO. http://hdl.handle.net/11250/2429012.

Li, Yingxia, Joo-Hyon Kang, Sim-Lin Lau, Masoud Kayhanian, and Michael K. Stenstrom. 2008. "Optimization of Settling Tank Design to Remove Particles and Metals." *J. Environ. Eng.* 134 (11): 885–894. https://doi.org/10.1061/(ASCE)0733-9372(2008)134:11(885).

Li, Yingxia, Sim-Lin Lau, Masoud Kayhanian, and Michael K. Stenstrom. 2006. "Dynamic Characteristics of Particle Size Distribution in Highway Runoff: Implications for Settling Tank Design." *Journal of Environmental Engineering* 132 (8): 852–861. https://doi.org/10.1061/(ASCE)0733-9372(2006)132:8(852).

———. 2005. "Particle Size Distribution in Highway Runoff." *Journal of Environmental Engineering* 131 (9): 1267–1276. https://doi.org/10.1061/(ASCE)0733-9372(2005)131:9(1267).

Lindholm, Oddvar, Svein Endresen, Sveinn Thorolfsson, Sveinung Sægrov, Guttorm Jakobsen, and Lars Aaby. 2008. *Veiledning i Klimatilpasset Overvannshåndtering. Norwegian Water report 162/2008.* Hamar. https://norskvann.no/index.php/kompetanse/va-bokhandelen/boker/produkt/801-a162-veiledning-i-klimatilpasset-overvannshandtering.

Makepeace, David K., Daniel W. Smith, and Stephen J. Stanley. 1995. "Urban Stormwater Quality: Summary of Contaminant Data." *Critical Reviews in Environmental Science and Technology* 25 (2): 93–139. https://doi.org/10.1080/10643389509388476.

Marsalek, J., G. Oberts, K. Exall, and M. Viklander. 2003. "Review of Operation of Urban Drainage Systems in Cold Weather: Water Quality Considerations." *Water Science and Technology* 48 (9): 11–20. https://doi.org/10.2166/wst.2003.0481.

Marsalek, J., Q. Rochfort, and L. Grapentine. 2005. "Aquatic habitat issues in urban stormwater management: Challenges and potential solutions." *International journal of ecohydrology hydrobiology* 5 (4): 269–279. ISSN: 1642-3593.

Meland, Sondre. 2010. "Ecotoxicological Effects of Highway and Tunnel Wash Water Runoff." PhD diss., Norwegian University of Life Sciences, Department of Plant and Environmental Sciences. http://hdl.handle.net/11250/190880.

———. 2018. "Forurensning i tunnelvaskevann – en studie av 34 veitunneler i Norge," no. 1, 54–65. https://vannforeningen.no/dokumentarkiv/forurensning-i-tunnelvaskevann-en-studie-av-34-veitunneler-i-norge/.

Miljø- og Fluidteknikk AS. 2020. *Downstream Defender Supersandfang Produktinformasjon.* https://mft.no/wp-content/uploads/DownstreamDefender-PI.pdf.

Monrabal-Martinez, Carlos, Thomas Meyn, and Tone Merete Muthanna. 2019. "Characterization and Temporal Variation of Urban Runoff in a Cold Climate - Design Implications for SuDS." *Urban Water Journal* 16 (6): 451–459. https://doi.org/10.1080/1573062X.2018.1536758.

NCCS, The Norwegian Centre for Climate Services. 2020. https://seklima.met.no/observations/.

NJCAT Technology Verification. 2015. *Downstream Defender Stormwater Treatment Device. Hydro International.* Technical report. http://www.njcat.org/uploads/newDocs/DDVerificationReport11117.pdf.

Norwegian Environment Agency. 2016. *Grenseverdier for klassifisering av vann, sediment og biota - revidert 30.10.2020.* https://www.miljodirektoratet.no/publikasjoner/2016/september-2016/grenseverdier-for-klassifisering-av-vann-sediment-og-biota/.

Nøst, Terje. 2019. "Monitoring of water resources in Trondheim 2019. Results.," 168. https://www.trondheim.kommune.no/vannovervaking/.

NPRA, Norwegian Public Roads Administration. 1997. *14.434 Kornfordeling ved våtsikting med slemmeanalyse.* https://www.vegvesen.no/s/vegnormaler/hb/014/Gamle_filer/14.43/014-434.pdf.

———. 2021a. *Trafikkdata Heimdalsmyra E6 Sør for Fjernvarmeanlegget.* https://www.vegvesen.no/trafikkdata/.

———. 2021b. *Trafikkdata Orstad.* https://www.vegvesen.no/trafikkdata/.

———. 2018. *Vegbygging NORMAL [Håndbok N200].* https://hdl.handle.net/11250/2760702.

Paus, Kim H. 2018. "Forslag til dimensjonerende verdier for trinn 1 i Norsk Vann sin tre-trinns strategi for håndtering av overvann." *Vannforeningen* 53 (1): 66–77. https://vannforeningen.no/dokumentarkiv/forslag-til-dimensjonerende-verdier-for-trinn-1-i-norsk-vann-sin-tre-trinns-strategi-for-handtering-av-overvann/.

Ranneklev, Sissel Brit, Thomas Correll Jensen, Anne Lyche Solheim, Sigrid Haande, Sondre Meland, Sondre Vikan, Turid Hertel-Aas, and Kjersti Wike Kronvall. 2016. "Water bodies vulnerability to runoff water from roads during the construction and operation phases," https://hdl.handle.net/11250/2672957.

Rossman, Lewis A. 2015. "Storm Water Management Model User's Manual Version 5.1." *U.S. Environmental Protection Agency,* 353. https://www.epa.gov/sites/production/files/2019-02/documents/epaswmm5_1_manual_master_8-2-15.pdf.

RStudio Team. 2019. *RStudio: Integrated Development Environment for R.* Boston, MA: RStudio, PBC. http://www.rstudio.com/.

Sansalone, John J., and Steven G. Buchberger. 1997a. "Characterization of Solid and Metal Element Distributions in Urban Highwaystormwater." *Water Sci Technolg* 36 (8-9): 155–160. https://doi.org/10.2166/wst.1997.0659.

———. 1997b. "Partitioning and First Flush of Metals in Urban Roadway Storm Water." *Journal of Environmental Engineering* 123, no. 2 (February): 134–143. https://doi.org/10.1061/(ASCE)0733-9372(1997)123:2(134).

Sansalone, John J., Steven G. Buchberger, and Margarete T. Koechling. 1995. "Correlations Between Heavy Metals and Suspended Solids in Highway Runoff: Implications for Control Strategies." *Transportation Research Record,* no. 1483, ISSN: 0361-1981.

Sansalone, John J., and Subbu-Srikanth Pathapati. 2009. "Particle Dynamics in a Hydrodynamic Separator Subject to Transient Rainfall-Runoff." *Water Resources Research* 45 (9). https://doi.org/10.1029/2008WR007661.

Sartor, James D., Gail B. Boyd, and Franklin J. Agardy. 1974. "Water Pollution Aspects of Street Surface Contaminants." *Journal (Water Pollution Control Federation)* 46 (3): 458–467. http://www.jstor.org/stable/25038149.

Selbig, Willliam R., Michael N. Fienen, Judy A. Horwatich, and Roger T. Bannerman. 2016. "The Effect of Particle Size Distribution on the Design of Urban Stormwater Control Measures." *Water* 8 (1): 17. https://doi.org/10.3390/w8010017.

Shrestha, Sushban, Xing Fang, and Wesley C. Zech. 2014. "What Should Be the 95th Percentile Rainfall Event Depths?" *Journal of Irrigation and Drainage Engineering* 140 (1): 06013002. https://doi.org/10.1061/(ASCE)IR.1943-4774.0000658.

Skjæveland Cementstøperi AS. https://www.skjeveland.no/.

Sorteberg, A., D. Lawrence, A. V. Dyrrdal, S. Mayer, K. Engeland, E. J. Førland, S. Johansen, N.K. Orthe, M. I. Sandvik, L Schlichting, R. G. Skaland, T. Skaugen, A. Voksø, K. Vormoor, and T. Væringstad. 2018. *Climatic Changes in Short Duration Extreme Precipitation and Rapid Onset Flooding - Implications for Design Values.* Technical report 1/2008. Norwegian Centre for Climate Services. https://klimaservicesenter.no/kss/om-oss/exprecflood.

Standards Norway. 1980. *Water analysis - Total residue, and total fixed residue in water, sludge and sediments. [NS 4764].* https://www.standard.no/no/Nettbutikk/produktkatalogen/Produktpresentasjon/?ProductID=134402.

———. 2005. *Water Quality. Determination of Suspended Solids.Method by Filtration through Glass Fibre Filters. [NS-EN 872].* https://www.standard.no/no/Nettbutikk/produktkatalogen/Produktpresentasjon/?ProductID=142811.

Storm Aqua AS. 2021. *FV505 Renseanlegg for vegvann, Sandnes. Renseløsning – Systembeskrivelse som-bygget.* Technical report. AvailableuponrequesttoStormAqua..

Strecker, Eric W., Marcus M. Quigley, Ben R. Urbonas, Jonathan E. Jones, and Jane K. Clary. 2001. "Determining Urban Storm Water BMP Effectiveness." *Journal of Water Resources Planning and Management* 127 (3): 144–149. https://doi.org/10.1061/(ASCE)0733-9496(2001)127:3(144).

Strømberg, Merethe Arntsen. 2020. "Sediment Removal Performance of a Hydrodynamic Vortex Separator." Master's Thesis, Norwegian University of Science and Technology. Available upon request to NTNU, IBM.

Tran, Duyen, and Joo-Hyon Kang. 2013. "Optimal Design of a Hydrodynamic Separator for Treating Runoff from Roadways." *Journal of Environmental Management* 116:1–9. ISSN: 0301-4797. https://doi.org/10.1016/j.jenvman.2012.11.036.

Tsihrintzis, Vassilios A., and Rizwan Hamid. 1997. "Modeling and Management of Urban Stormwater Runoff Quality: A Review." *Water Resources Management* (Dordrecht, Netherlands) 11 (2): 136–164. https://doi.org/http://dx.doi.org/10.1023/A:1007903817943.

Tuccillo, M. 2006. "Size Fractionation of Metals in Runoff from Residential and Highway Storm Sewers." *Science of The Total Environment* 355 (1-3): 288–300. https://doi.org/10.1016/j.scitotenv.2005.03.003.

Vannforskriften. 2006. *Forskrift Om Rammer for Vannforvaltningen.* https://lovdata.no/forskrift/2006-12-15-1446.

Vijayan, Arya, Heléne Österlund, Jiri Marsalek, and Maria Viklander. 2019. "Laboratory Melting of Late-Winter Urban Snow Samples: The Magnitude and Dynamics of Releases of Heavy Metals and PAHs." *Water, Air, & Soil Pollution* 230 (8): 182. https://doi.org/10.1007/s11270-019-4201-2.

Viklander, M., J. Marsalek, P.-A. Malmquist, and W.E. Watt. 2003. "Urban Drainage and Highway Runoff in Cold Climates: Conference Overview." *Water Science and Technology* 48 (9): 1–10. https://doi.org/10.2166/wst.2003.0479.

Viklander, Maria. 1998. "Snow Quality in the City of Luleå, Sweden — Time-Variation of Lead, Zinc, Copper and Phosphorus." *Science of The Total Environment* 216 (1): 103–112. https://doi.org/10.1016/S0048-9697(98)00148-X.

Wang, Weisheng, Bei Wen, Shuzhen Zhang, and Xiao-Quan Shan. 2003. "Distribution of Heavy Metals in Water and Soil Solutions Based on Colloid-Size Fractionation." *International Journal of Environmental Analytical Chemistry* 83 (5): 357–365. https://doi.org/10.1080/0306731031000104704.

Wang, WH, MH Wong, S Leharne, and B Fisher. 1998. "Fractionation and biotoxicity of heavy metals in urban dusts collected from Hong Kong and London." *Environmental geochemistry and health* 20 (4): 185–198. https://doi.org/10.1023/A:1006530300522.

Westerlund, Camilla, and Maria Viklander. 2006. "Particles and associated metals in road runoff during snowmelt and rainfall." *Science of The Total Environment* 362 (1): 143–156. ISSN: 0048-9697. https://doi.org/10.1016/j.scitotenv.2005.06.031.

Westerlund, Camilla, Maria Viklander, and Magnus Bäckström. 2003. "Seasonal Variations in Road Runoff Quality in Luleå, Sweden." *Water Science and Technology* 48 (5): 93–1003. https://doi.org/10.2166/wst.2003.0501.

Wilson, Matthew A., Omid Mohseni, John S. Gulliver, Raymond M. Hozalski, and Heinz G. Stefan. 2009. "Assessment of Hydrodynamic Separators for Storm-Water Treatment." *Journal of Hydraulic Engineering* 135 (5): 383–392. https://doi.org/10.1061/(ASCE)HY.1943-7900.0000023.

A Appendix A - Sampling setup

Setup Trondheim

(1)

(2)

(3)

(4)

Figure A1: Pictures from the setup of the samplers at the hydrodynamic vortex separator. Pictures: Kristine Bergseng

(1) The sampelers are installed in the upstream and downstram manhole with steel chains.
(2) Upstream manhole with the AV-module installed inside the inlet pipe.
(3) The low profile AV-module are installed inside the pipes with a spring ring.
(4) The strainer (red ring) are placed longitudinally downstream the AV-sensor (arrow).

Setup Sandnes

(1)

(2)

(3)

(4)

Figure A2: Pictures from the setup of the inlet and outlet samplers at the modular sedimentation system (MSS). Pictures: Lars Møller-Pedersen.

(1) Placement of the inlet sampler.
(2) Setup of suction line inside the inlet pipe.
(3) Sampler in the outlet manhole.
(4) Setup of suctionline inside the outlet pipe.

Proposal for location of hydrodynamic vortex separator

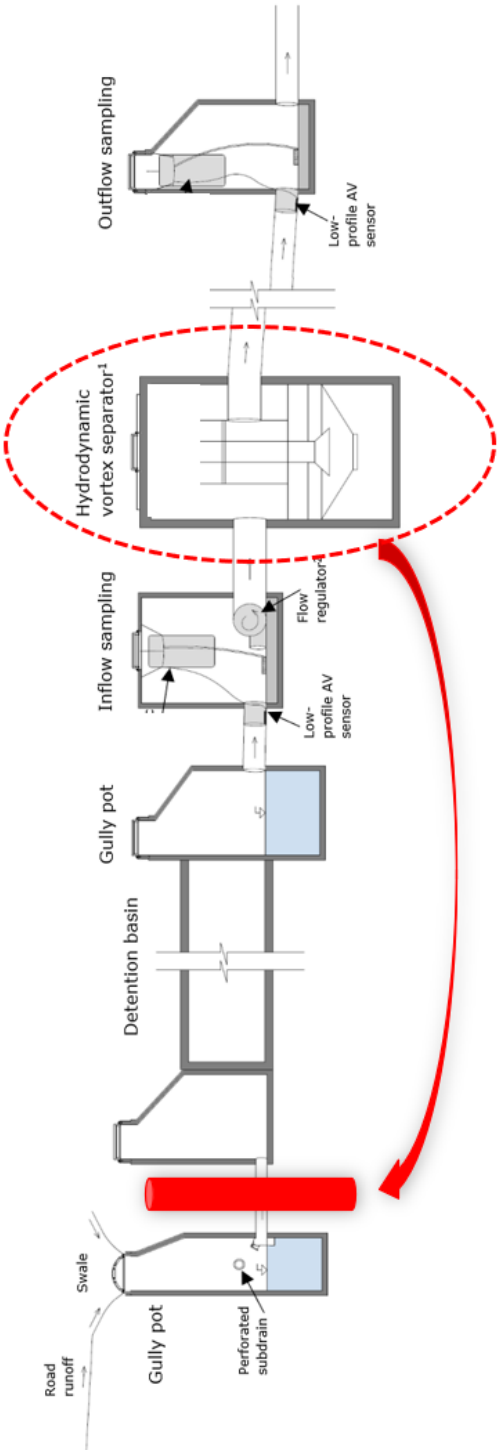

Figure A3: Suggestion to move the HVS further upstream the treatment train. The figure is modified from Merethe Arntsen Strømberg (2020); "Sediment Removal Performance of a Hydrodynamic VortexSeparator."

B Appendix B - Note metal fractionation

Review of size fractionation used in metal concentration analyses for runoff in Scandinavia

Kristine Bergseng, 25.02.2021
Note

Department of Civil and Environmental Engineering.
Norwegian University of Science and Technology

Introduction

The focus and interest on the water quality of road runoff have increased over the last decades. In report number 46 from Vegdirektoratet (Åstebøl et al., 2011) knowledge gaps related to water pollution from tunnel wash water and road runoff are identified. Among the questions that need to be answered is how toxic this runoff is. This question includes which substances and fractions (dissolved, colloidal, and particle-bound) this toxicity is attached. In this report, the division between particulate and dissolved are bigger or smaller than 0.45 μm.

Runoff draining transports matter in a wide range of sizes. Heavy metals are associated with these particles, with increased concentrations in finer particle sizes (Sansalone and Buchberger, 1997). In the pioneering studies, few studies are in the same field, which means that few examples are to follow. Therefore, it has not been a clear standard of defining the size range of particulate, colloidal, dissolved, and truly dissolved fractions. This makes some studies difficult to compare because the fractions overlap. By using the same classification of fractions, more studies can be compared. This can result in a greater understanding of the road runoff. Therefore, this review aims to answer the following question:

- What are the pore sizes of the filters used to fraction the matter when analyzing metal concentrations in Scandinavia?
- How are the different fractions defined?

This review presents several different studies done in Scandinavian countries to show different practices related to fractionation.

Results

Summaries of a selection of studies and reports done in Scandiavia analysing metal consentration in road runoff (RR) and tunnel wash water (TWW). Abbreviations in the table; Colloidal (C), Dissolved (D), Particulate (P), and Truly dissolved (TD).

Title	Reference	Country	Runoff type	Analysis	Filter size
Ecological risk assessment with Biotic Ligand Model	Johansen and Thygesen, 2013	Norway, (Oslo, Viken)	RR, TWW	P, D	0.45 μm
The effects of detergent (TK601) on the mobility of metals during sedimentation of tunnel wash water from the nordbytunnel at a motorway (E6) in Norway. - A laboratory experiment.	Aasum, 2013	Norway, (Viken)	TWW	P, D, C, TD	0.45 μm, 10 kDa
Laboratory tests - treatment of tunnel wash water from the Nordby tunnel	Garshol et al., 2016	Norway, (Viken)	TWW	P, D, C, TD	0.45 μm, 10 kDa
Ecotoxicological effects of highway and tunnel wash water runoff	Meland, 2010	Norway, (Viken)	RR, TWW	P, D, C, TD	0.45 μm, 10 kDa
Laboratory Melting of Late-Winter Urban Snow Samples: The Magnitude and Dynamics of Releases of Heavy Metals and PAHs	Vijayan et al., 2019	Sweden, (Luleå, Umeå)	RR	P, C, TD	0.45 μm, 3 kDa
A study of size fractions of metals in sedimented tunnel wash water	Kowollik, 2020	Norway, (Oslo, Viken)	TWW	P, D, C, TD	1.2 μm, 0.45 μm, 3 kDa
Snow quality in the city of Lulea, Sweden - time variation of lead, zinc, copper and phosphorus.	Viklander, 1998	Sweden, (Luleå)	RR	P, D	0.45 μm
Contribution of coarse particles from road surfaces to dissolved and particle-bound heavy metal loads in runoff: A laboratory leaching study with synthetic stormwater	Borris et al., 2016	Sweeden	RR	P, D	0.45 μm

Title	Reference	Country	Runoff type	Analysis	Filter size
Metal size distribution in rainfall and snowmelt-induced runoff from three urban catchments	Lindfors et al., 2020	Sweeden, (Umeå)	RR	P, D, C, TD	0.45 μm, 3 kMWCO $\sim$ 1 nm
Characterization and temporal variation of urban runoff in a cold climate - design implications for SuDS	Monrabal-Martinez et al., 2019	Norway, (Trond-heim)	RR	P, C, TD	1.2 μm, 1 kDa
Dual Porosity Filtration for treatment of stormwater runoff: first proof of concept from Copenhagen pilot plant	Jensen et al., 2011	Denmark, (Copen-hagen)	RR	-	-
Treatment efficiency of a wet detention pond combined with filters of crushed concrete and sand: a Danish full-scale study of stormwater	Sønderup et al., 2015	Denmark	RR	P, D	1.2 μm
Heavy metal composition in stormwater and retention in ponds dependent on pond age, design and catchment type	Egemose et al., 2015	Denmark, (Aaben-raa)	RR	P, D	1.2 μm
Evaluation of the accumulation of sediment and heavy metals in a storm-water detention pond	Färm, 2002	Sweden, (Väst-erås)	RR	P, D	0.45 μm
Urban impact on water bodies in the Luleå area, northern Sweden, and the role of redox processes	Rentz and Öhlander, 2012	Sweden, (Luleå)	RR	P	0.22 μm
Seasonal variations in road runoff quality in Luleå, Sweden	Westerlund et al., 2003	Sweden, (Luleå)	RR	P, D	0.45 μm
Heavy metal concentrations and toxicity in water and sediment from stormwater ponds and sedimentation tanks	Karlsson et al., 2010	Sweden	RR	P, D	0.45 μm

The paper written by Johansen and Thygesen, 2013 analyzed the total and soluble metal concentrations. The study includes basins along the road stretches E6 Gardermoen - Eidsvoll,

E18 Askim - Mysen, E18 Drammen - Holmestrand, and within the city of Oslo. The soluble concentration is defined as the fraction that goes through a 0.45 μm cellulose acetate membrane.

Aasum, 2013 was studying tunnel wash water (TWW) from Nordbytunnelen in his Master's Thesis. Three fractions were used; particulate, colloidal, and soluble. The particulate fraction is removed from the water when filtering through a 0.45 μm filter. The colloidal fraction has a range of 0.45 μm to 10 kDa. The fraction that goes through the 10 kDa filter is defined as soluble and consists of low molecular mass (LMM). This same fractioning was used in NPRA report number 521 (Garshol et al., 2016) and in the Ph.D. thesis of Meland, 2010, which was both doing analyses of the tunnel wash water in the same tunnel.

Vijayan et al., 2019 did laboratory snow melting experiments of late-winter snow samples from highway snowbanks. Three different fractions were analyzed for metal concentrations: total, dissolved, and truly dissolved. The dissolved and particulate fractions were separated by a 0.45 μm filter. The fraction passing through the 3 kDa ultrafilter is defined as the truly dissolved fraction. Kowollik (2020) used the same fractionation in addition to a filter with size 1.2 μm to distinguish between fine and coarse particles. The small particles are defined as the range between 1.2 μm to 0.45 μm. An ongoing study regarding the treatment of tunnel wash water led by Associate Professor Thomas Meyn at NTNU uses the same fractionation as Kowollik (2020). The study is an extension of the Nordic Road Water (NORWAT) program.

Monrabal-Martinez et al., 2019 analyzed metals in the fractions suspended matter ($>$1.2 μm), colloids including fine particles ($<$1.2 μm and $>$1 kDa), and dissolved matter ($<$1 kDa) for road runoff in Trondheim.

Jensen et al., 2011 does not fraction filter the samples before analyzing for the metal concentration. This is found in many studies, but this study is presented as an example.

Sønderup et al., 2015 does not describe the method in detail, but it is understood that the particulate and dissolved fractions are distinguished by a filter size 1.2 μm. This differs from the others. Egemose et al., 2015 did use filters with the same pore size for fractioning.

Viklander, 1998, Borris et al., 2016, Westerlund et al., 2003, Karlsson et. al. Karlsson et al., 2010 and Färm, 2002, all based in Sweeden, did all fraction with a 0.45 μm filter. Rentz and Öhlander, 2012 used a filter with nominal pore size of 0.22 μm to.

Discussion and conclusion

In the studies in this review the following filter sizes has been used; 1.2 μm, 0.45 μm, 0.22 μm, 10 kDa, 3 kDa, 1 kDa, and 3 kMWCO. In studies where only one type of filter are used the sizes are 1.2 μm, 0.45 μm, and 0.22 μm. When the smaller ultra filters (10 kDa - 1 nm) are used, the colloidal fraction is defined as the matter held back, but goes through a 1.2 μm or 0.45 μm filter. The matter passing through an ultrafilter are defined as low molecular mass (LMM) (Aamaas et al., 2018) or truly dissolved (Vijayan et al., 2019)(Kowollik, 2020)(Monrabal-Martinez et al., 2019).

It seems like it is widespread to distinguish the particulate and dissolved fractions of metals by filtration through a 0.45 μm filter, where the metals in the filtrate are considered the dissolved fraction. This is a fractionation that seems to be universal in the field, also outside Scandinavia (Sansalone and Buchberger, 1997)(Tuccillo, 2006).

From an overview of the studies, the following fractionation can be used: Particulate fraction (coarse particles $>$ fine particles) $>$ dissolved particles (colloidal fraction $>$ truly dissolved). The 1.2 μm filter are distinguishing the particulate fraction into coarse particles and fine particles. Further, as mentioned above, the 0.45 μm separates the particulate and dissolved fraction. The dissolved fraction consists of a colloidal fraction, and the smallest can be defined as truly dissolved. In the studies, the colloidal fraction is defined as the fraction between 0.45 μm and 10 kDa, 3 kDa, 1 kDa, or 1 nm. The lower limit of the fractioning is varying in the studies. At the studies at NMBU 10 kDa, while at some past and ongoing studies at NTNU 3 kDa are used. Where this limit should be set can be further discussed, but for the master's thesis to be written in the spring of 2021, it is appropriate to use the same filter size as other studies at the university.

For the analysis of metal concentrations in this study, filters in the sizes 1.2 μm, 0.45 μm, and 3 kDa are preferred to be used. By using these filters, it will be easy to compare to other studies for most fractions. The fractionating will then be as seen in Table B.1.

Table B.1: Suggested fractionation method when analyzing metal concentrations for different size ranges. LMM is the abbreviation for low molecular mass, which is truly dissolved in the water.

Fraction		Range
Particulate	Coarse particle	$>$ 1.2 μm
	Fine particle	1.2 μm - 0.45 μm
Dissolved	Colloidal	0.45 μm - 3 kDa
	Truly dissolved (LMM)	$<$3 kDa

Together with other studies at NTNU and citeAryaSnowMelt there can be a beginning of data series that uses the same fractionation.

References

Aamaas, Borgar, Asbjørn Aaheim, Kristina Alnes, Bob van Oort, Halvor Dannevig, and Torunn Hønsi. 2018. *Oppdatering Av Kunnskap Om Konsekvenser Av Klimaendringer i Norge.* Technical report M-1209. Oslo. https://www.miljodirektoratet.no/publikasjoner/2019/januar-2019/oppdatering-av-kunnskap-om-konsekvenser-av-klimaendringer-i-norge/.

Aasum, Jon-Henning. 2013. *The Effects of Detergent (TK601) on the Mobility of Metals during Sedimentation of Tunnel Wash Water from the Nordbytunnel at a Motorway (E6) in Norway. - A Laboratory Experiment.* http://hdl.handle.net/11250/190856.

Åstebøl, Svein Ole, Thorkild Hvitved-Jacobsen, and Jesper Kjølholt. 2011. *NORWAT - Nordic Road Water Road and Water Pollution. A Review and Identification of Research Gaps.* http://hdl.handle.net/11250/2582823.

Borris, Matthias, Heléne Österlund, Jiri Marsalek, and Maria Viklander. 2016. "Contribution of Coarse Particles from Road Surfaces to Dissolved and Particle-Bound Heavy Metal Loads in Runoff: A Laboratory Leaching Study with Synthetic Stormwater." *Science of The Total Environment* 573. https://doi.org/10.1016/j.scitotenv.2016.08.062.

Egemose, Sara, Melanie J. Sønderup, Anna Grudinina, Anders S. Hansen, and Mogens R. Flindt. 2015. "Heavy Metal Composition in Stormwater and Retention in Ponds Dependent on Pond Age, Design and Catchment Type." *Environmental Technology* 36 (8): 959–969. https://doi.org/10.1080/09593330.2014.970584.

Färm, C. 2002. "Evaluation of the Accumulation of Sediment and Heavy Metals in a Storm-Water Detention Pond." *Water Science and Technology* 45 (7): 105–112. https://doi.org/10.2166/wst.2002.0122.

Garshol, Frøydis K., Maria Magdalena Rebo Estevez, Ashish Sahu, Mona Eftekhar Dadkhah, Subhash S Rathnaweera, Liv Bruås Henninge, Arne Lundar, Ocelie Kjønnø, Michael S Nilan, and Pascale Stang. 2016. *Laboratory Tests - Treatment of Tunnel Wash Water from the Nordby Tunnel.* NPRA Reports 521. Norwegian Public Roads Administration. https://hdl.handle.net/11250/2671290.

Jensen, Marina B, Karin Cederkvist, Per E R Bjerager, and Peter E Holm. 2011. "Dual Porosity Filtration for Treatment of Stormwater Runoff: First Proof of Concept from Copenhagen Pilot Plant." *Water Science,* 1547–1557. https://doi.org/https://doi.org/10.2166/wst.2011.186.

Johansen, Susanne Lund, and Helene Thygesen. 2013. *Ecological Risk Assessment with Biotic Ligand Model.* Technical report 230. Norwegian Public Roads Administration. https://hdl.handle.net/11250/2657883.

Karlsson, Kristin, Maria Viklander, Lian Scholes, and Mike Revitt. 2010. "Heavy Metal Concentrations and Toxicity in Water and Sediment from Stormwater Ponds and Sedimentation Tanks." *Journal of Hazardous Materials* 178 (1): 612–618. https://doi.org/10.1016/j.jhazmat.2010.01.129.

Kowollik, Helene Sundnes. 2020. "A Study of Size Fractions of Metals in Sedimented Tunnel Wash Water." Master's thesis.

Lindfors, Sarah, Heléne Österlund, Lian Lundy, and Maria Viklander. 2020. "Metal Size Distribution in Rainfall and Snowmelt-Induced Runoff from Three Urban Catchments." *Science of The Total Environment* 743:140813. https://doi.org/10.1016/j.scitotenv.2020.140813.

Meland, Sondre. 2010. "Ecotoxicological Effects of Highway and Tunnel Wash Water Runoff." PhD diss., Norwegian University of Life Sciences, Department of Plant and Environmental Sciences. http://hdl.handle.net/11250/190880.

Monrabal-Martinez, Carlos, Thomas Meyn, and Tone Merete Muthanna. 2019. "Characterization and Temporal Variation of Urban Runoff in a Cold Climate - Design Implications for SuDS." *Urban Water Journal* 16 (6): 451–459. https://doi.org/10.1080/1573062X.2018.1536758.

Rentz, Ralf, and Björn Öhlander. 2012. "Urban Impact on Water Bodies in the Luleå Area, Northern Sweden, and the Role of Redox Processes." *Hydrology Research* 43 (6): 917–932. https://doi.org/10.2166/nh.2011.167.

Sansalone, John J., and Steven G. Buchberger. 1997. "Characterization of Solid and Metal Element Distributions in Urban Highwaystormwater." *Water Sci Technolg* 36 (8-9): 155–160. https://doi.org/10.2166/wst.1997.0659.

Sønderup, Melanie J., Sara Egemose, Timm Bochdam, and Mogens R. Flindt. 2015. "Treatment Efficiency of a Wet Detention Pond Combined with Filters of Crushed Concrete and Sand: A Danish Full-Scale Study of Stormwater." *Environmental Monitoring and Assessment* 187 (12): 758. https://doi.org/10.1007/s10661-015-4975-7.

Tuccillo, M. 2006. "Size Fractionation of Metals in Runoff from Residential and Highway Storm Sewers." *Science of The Total Environment* 355 (1-3): 288–300. https://doi.org/10.1016/j.scitotenv.2005.03.003.

Vijayan, Arya, Heléne Österlund, Jiri Marsalek, and Maria Viklander. 2019. "Laboratory Melting of Late-Winter Urban Snow Samples: The Magnitude and Dynamics of Releases of Heavy Metals and PAHs." *Water, Air, & Soil Pollution* 230 (8): 182. https://doi.org/10.1007/s11270-019-4201-2.

Viklander, Maria. 1998. "Snow Quality in the City of Luleå, Sweden — Time-Variation of Lead, Zinc, Copper and Phosphorus." *Science of The Total Environment* 216 (1): 103–112. https://doi.org/10.1016/S0048-9697(98)00148-X.

Westerlund, Camilla, Maria Viklander, and Magnus Bäckström. 2003. "Seasonal Variations in Road Runoff Quality in Luleå, Sweden." *Water Science and Technology* 48 (5): 93–1003. https://doi.org/10.2166/wst.2003.0501.

C Appendix C - Model data and calibration script

Storm Water Management Model (SWMM)

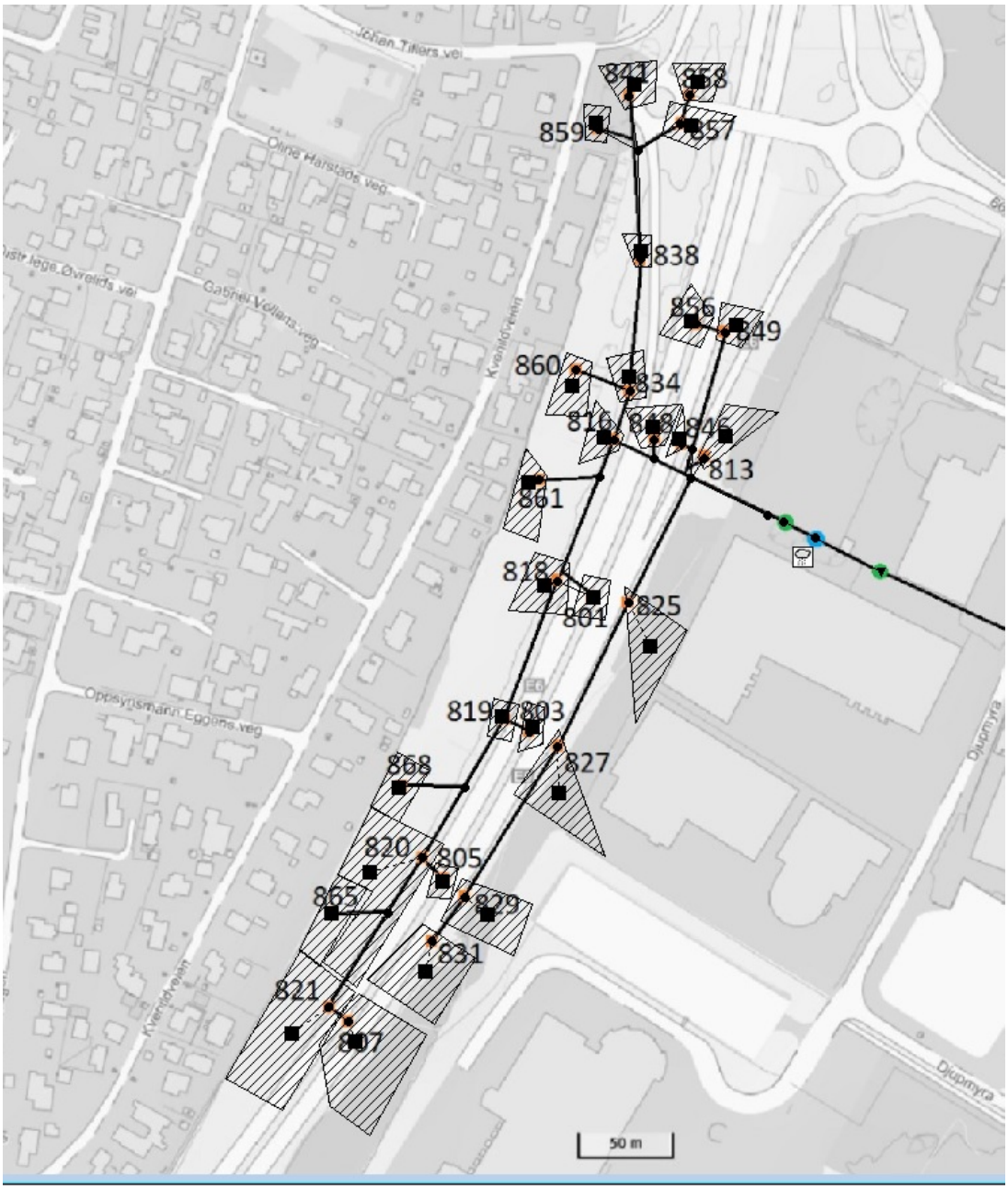

A screenshot of the Storm Water Management Model of the HVS study site. The green dots are the upstream and downstream manhole, respectively. The HVS (RK810) are represented with the blue spot.

Subcatchment information from the SWMM model.

Outlet	Area	% Imperv	Width	Slope
SF807	0.1532	83.9	110.41	3
SF821	0.1615	69.1	112.18	40
SF865	0.2758	60.0	139.16	3
SF820	0.1238	68.5	68.56	40
SF868	0.2151	60.0	71.85	3
SF819	0.1574	68.2	84.45	40
SF803	0.1086	83.4	81.77	3
SF801	0.1294	85.4	79.25	40
SF805	0.1024	84.2	72.23	3
SF818	0.1709	67.8	77.94	40
SF860	0.2626	60.0	82.03	3
SF834	0.0993	71.2	66.2	50
SF838	0.1468	75.3	75.71	50
SF859	0.3915	60.0	119.31	3
SF841	0.0274	71.3	19.31	3
SF858	0.0323	91.1	29.58	3
SF857	0.0183	94.9	29.82	1
SF861	0.5479	60.0	166.9	3
SF816	0.2723	68.8	81.21	50
SF848	0.1329	85.2	81.35	3
SF856	0.1247	86.1	69.81	3
SF849	0.0481	72.1	31.39	6
SF846	0.0972	75.9	62.08	6
SF813	0.0596	68.2	52.06	6
SF825	0.3503	74.0	88.40	3
SF827	0.1542	68.9	79.22	3
SF829	0.0537	67.1	30.01	3
SF831	0.2837	68.0	147.68	3

Default parameters used in the SWMM-model

Default Parameters	
S-Imperv	0.05
S-Perv	0.05
Param 1	100
Param 2	30
Param 3	4
Param 4	7
Param 5	0

R-script for Calibration of SWMM-model

```
#This is a code for calibrating a SWMM model
#The author of the script is Elhadi Mohsen Hassan Abdalla, NTNU.
#The script is applied to the SWMM model for the HVS and the measured diver data by Kristine Bergseng
#The script is made for SWMM version 3.6.1

library(swmmr) #Allows R to run SWMM
library(DEoptim)
library(zoo)
library(lubridate)
library(readxl)
inp_file <- "Trondheim_modell_parameter.inp" #File directory to .inp file
inp <- read_inp(inp_file) # SWMM has .inp file
obs_wl <- read_excel("Oppstroms.xlsx") #The diver data
obs_wl <- obs_wl$WaterLevel_filter/100 #Converting water levels from cm to m in diver data.
obsWL  <- unname(tapply(obs_wl, (seq_along(obs_wl)-1) %/% 5, mean)) # 5 minute data

obj_fun <- function(param,inp_file,obsWL) {
  inp <- read_inp(inp_file)   # set new parameters and update inp object
  inp$subareas <- transform(
    inp$subareas,
    `N-Imperv` = rep(param[1],28), #Mannings value for impervious surface
    `N-Perv` = rep(param[2],28)) #Mannings value for pervious surface

  # write new inp file to disk
  tmp_inp <- tempfile()
  write_inp(inp, tmp_inp)

  # run SWMM with new parameter set
  swmm_files <- suppressMessages(run_swmm(tmp_inp, stdout = NULL))

  # remove files when function exits to avoid heavy disk usage
  on.exit(file.remove(unlist(swmm_files)))

  sim <- read_out(
    file = swmm_files$out,
    iType =2,
    object_name = "O812-O811",
    vIndex = 1)[["O812-O811"]][["average_water_depth"]]

```

```
  sim <- sim[c(1321:7752),] #Adjust length of model data set
  sim <- as.array(coredata(sim))

  #Making equal lengths of data set
  if(length(obsWL)-length(sim) == 0){
    KGE_Q <- hydroGOF::NSE(sim = as.array(sim),obs=as.matrix(
   obsWL[1:length(obsWL)]))}
  if(length(obsWL)-length(sim) == 1){
    KGE_Q <- hydroGOF::NSE(sim = as.array(sim),obs=as.matrix(
   obsWL[1:(length(obsWL)-1)]))}
  if(length(obsWL)-length(sim)== 2){
    KGE_Q <- hydroGOF::NSE(sim = as.array(sim),obs=as.matrix(
   obsWL[2:(length(obsWL)-1)]))}

  #VOL <- 1-abs(KGE_Q/100)
  KGE_Q1 <- ifelse(is.na(KGE_Q)==TRUE,-999,KGE_Q)

  #plot(Qobs,type = "l",col="blue",lwd=2)
  #lines(sim,col="red",lwd=2)
  return(KGE_Q1*-1 }

calibration_res <- DEoptim(
  fn = obj_fun,
  lower = c(0.1,0.1), #Lover limit of N-imperv and N-perv
  upper = c(0.4, 0.5), #Upper limit of N-imperv and N-perv
  DEoptim.control(trace=TRUE,parallelType=1,packages=c("swmmr","
   zoo"),
                  parVar=c("read_inp","write_inp","read_out","run
   _swmm","coredata"),itermax = 4000),
  inp_file = inp_file,
  obsWL = obsWL)
```

D Appendix D - Sediment sampling

Sampling of gully pot sediments

(1)

(2)

(3)

(4)

Pictures from the sampling of gully pots in the upstream system of the hydrodynamic vortex separator. Pictures: Kristine Bergseng and Christoffer Kjelsberg

(1) The vacuum vehicle was suctioning up the water over the sediments before sampling.
(2) The van veen grab was lowered into the center of the gully pot after the water was removed.
(3) The van veen grab lifted up full of sediments.
(4) The sediments were poured into one-liter plastic bottles.

The gully pots upstream of the hydrodynamic vortex separator had to be sampled at night due to HSE. To be able to sample at the highway, an impact protection vehicle had to secure the site. Gully pots in between northbound and southbound lanes could not be sampled because two impact protection vehicles would have been necessary. The exit and access ramp in the area could not be closed; therefore, these gully pots could not be sampled.

E Appendix E - Summary of lab analyses of water

Hydrodynamic Vortex Separator - Summary of lab analyses of water samples

HVS - 25th of February event

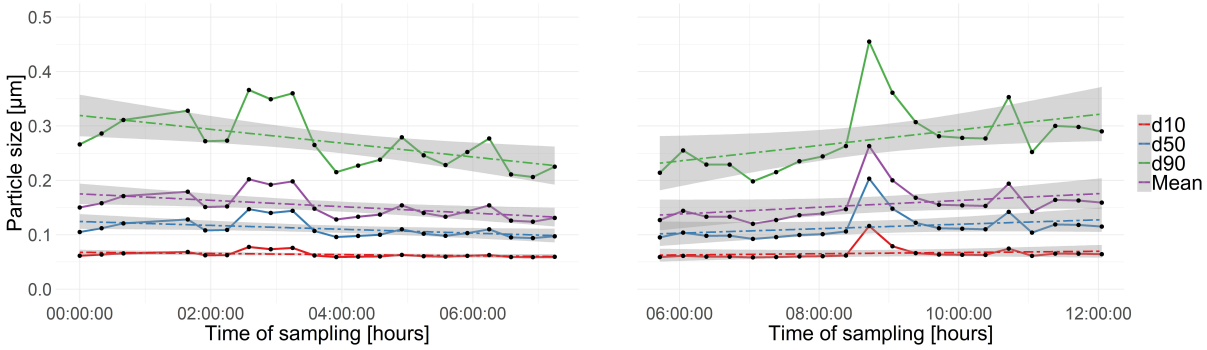

The upstream (left) and downstream (right) plots of the mean, d10, d50 and d90 particles in the 25th of February event. The dotted line represents the trend line.

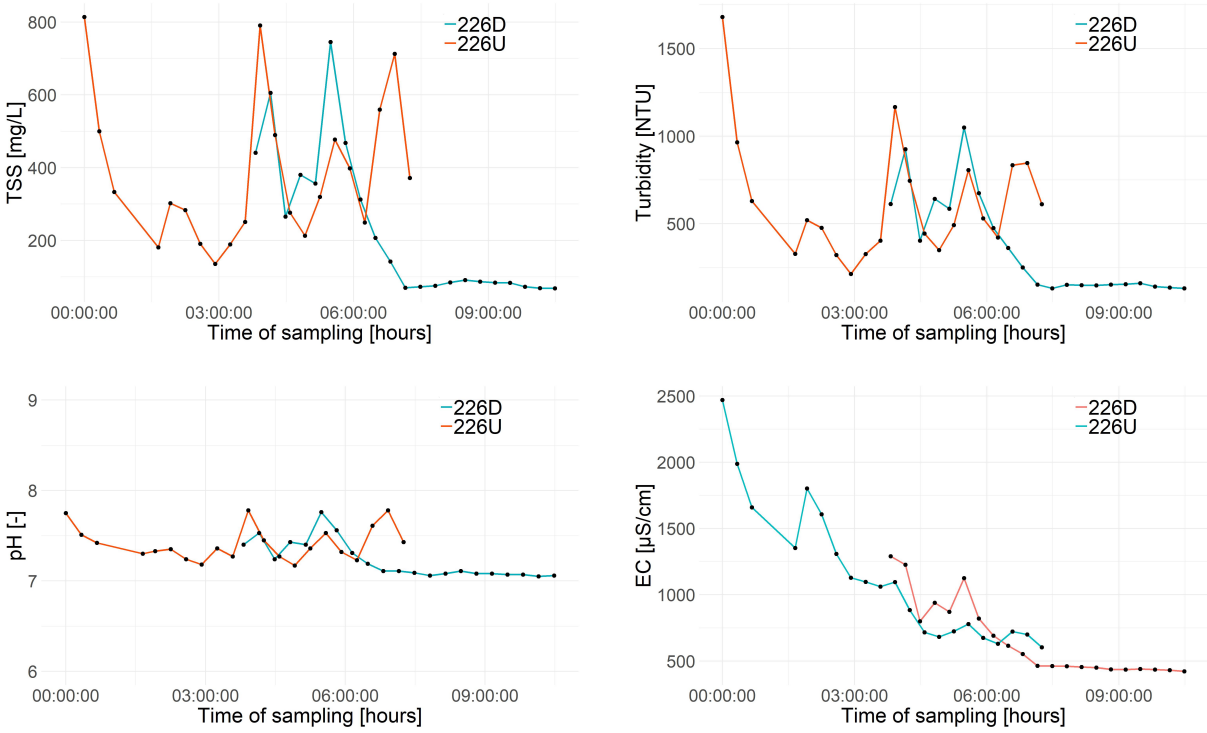

Results of lab analyses for TSS, Turbidity, pH and EC for the 25th of February event. In the legend 226D represent the downstream and 226U the upstream flow.

HVS - 6th of March event

Results of the lab analyses of PSD, TSS, turbidity, pH and EC for the 6th of March event.

		Upstream				Downstream		
Time of sampling [hours]		00:00	00:23	00:43	01:03	02:04	02:15	02:35
PSD	Mean [μm]	0.150	0.168	0.188	0.176	0.257	0.223	0.180
	d10 [μm]	0.062	0.065	0.070	0.067	0.107	0.088	0.068
	d50 [μm]	0.108	0.118	0.134	0.124	0.192	0.163	0.128
	d90 [μm]	0.271	0.307	0.345	0.323	0.451	0.402	0.330
TSS [mg/L]		60	60	58	-	44.1	46.2	-
Turbidity [NTU]		85	90	101	-	77.4	81.7	-
pH [-]		7.37	7.33	7.32	-	7.47	7.46	-
EC [μS/cm]		1395	1407	1507	-	1516	1544	-

HVS - 22th of March event

TSS upstream = 80 mg/L
TSS downstream = 78 mg/L

HVS - 21st of April event

Results of the lab analyses of PSD, TSS, turbidity, pH and EC for the 21st of April event.

		Upstream	Downstream
Time of sampling [hours]		00:00	00:23
PSD	Mean [μm]	0.129	0.108
	d10 [μm]	0.059	0.057
	d50 [μm]	0.095	0.087
	d90 [μm]	0.217	0.171
TSS [mg/L]		62	7.3
Turbidity [NTU]		97	15.8
pH [-]		7.32	7.39
EC [μS/cm]		747	637

HVS - 20th of March event

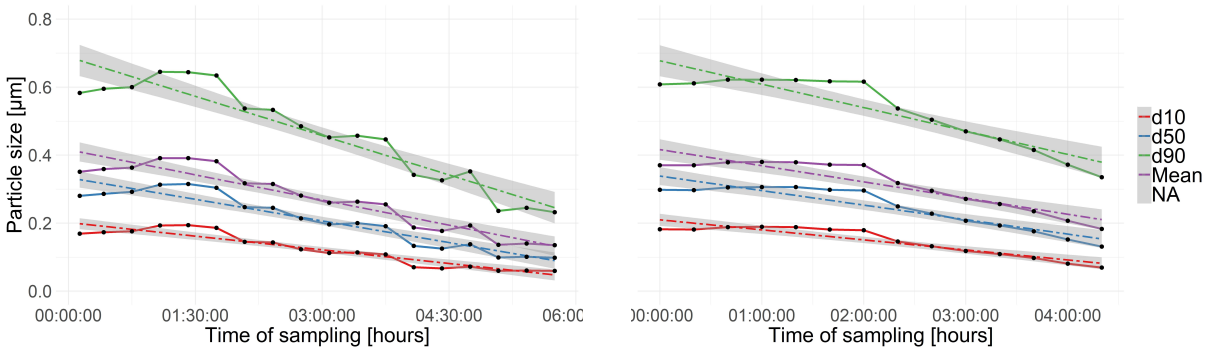

The upstream (left) and downstream (right) plots of the mean, d10, d50 and d90 particles in the 20th of March event. The dotted line represents the trend line.

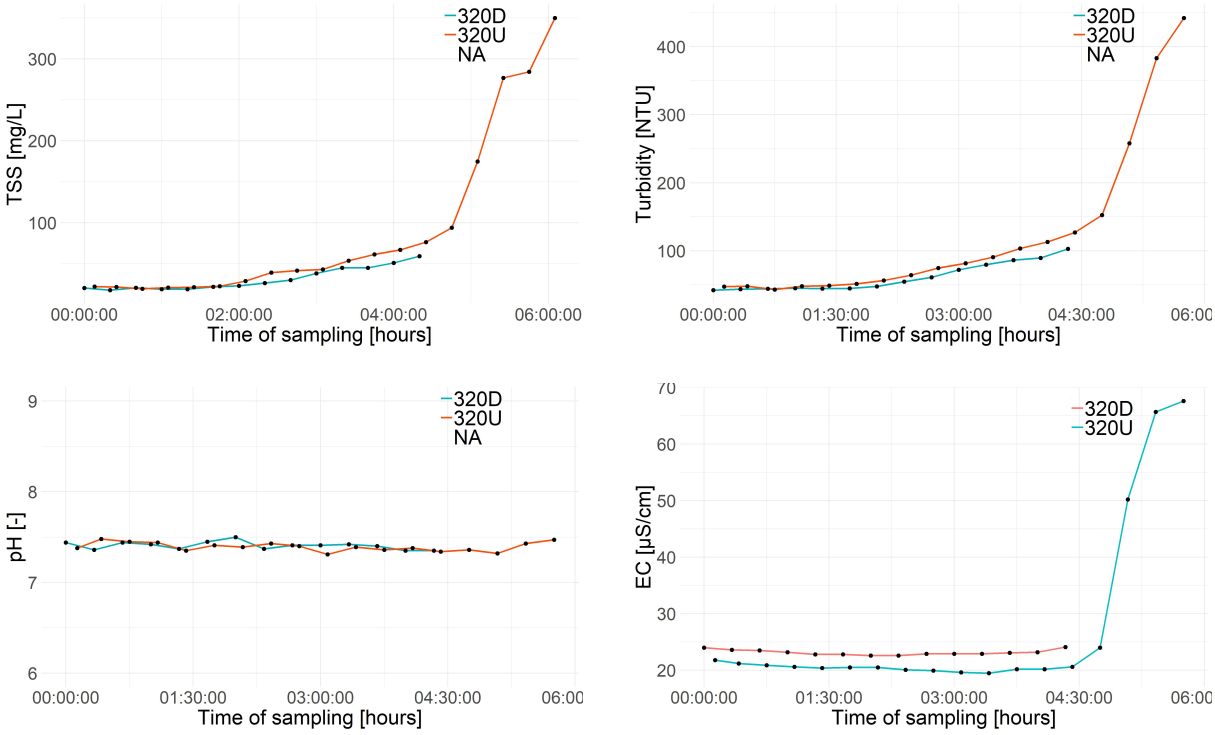

Results of lab analyses for the 20th of March event. The black point are the actual sampling results. In the legend 320D represent the downstream and 320U the upstream flow. NA can be ignored.

Modular Sedimentation System- Summary of lab analyses of water samples

MSS - 28th of March event

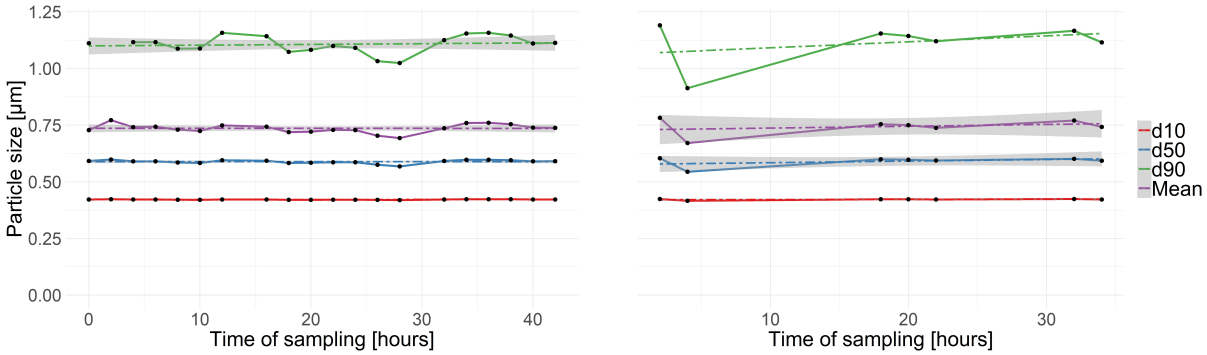

The upstream (left) and downstream (right) plots of the mean, d10, d50 and d90 particles in the 28th of March event. The dotted line represents the trend line.

MSS - 8th of April event

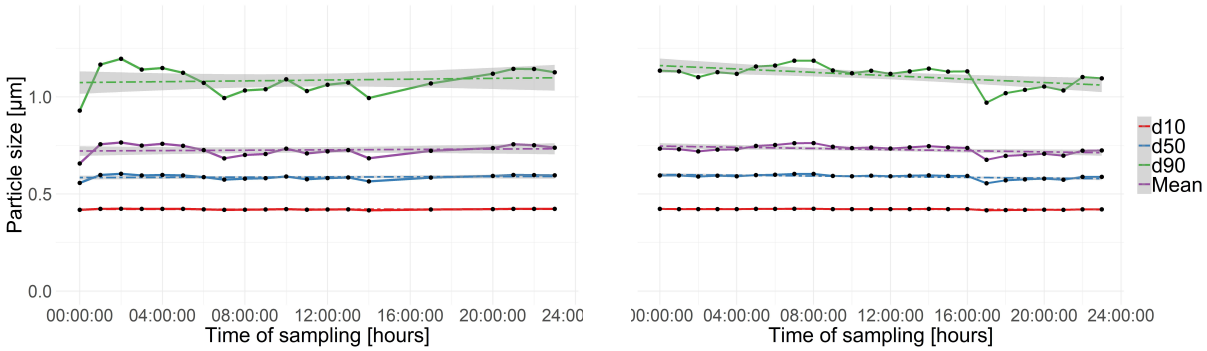

The upstream (left) and downstream (right) plots of the mean, d10, d50 and d90 particles in the 8th of April event. The dotted line represents the trend line.

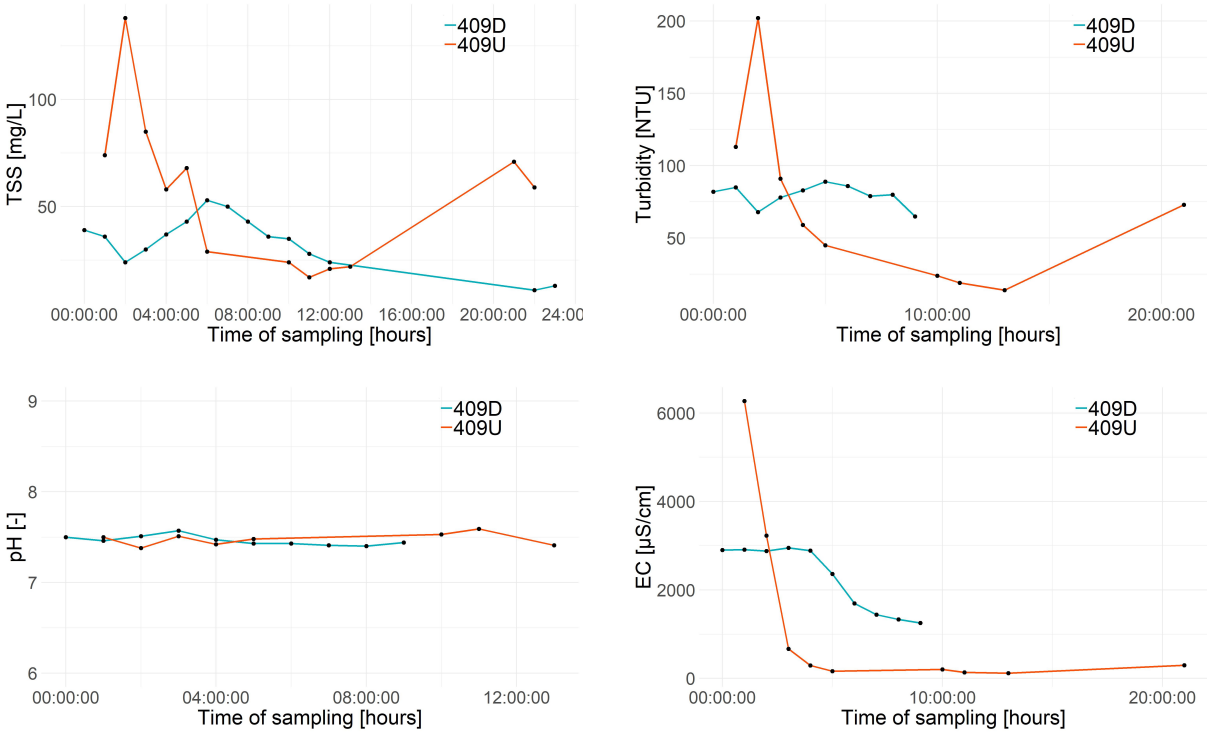

Results of the lab analyses from the 8th of April event. The black points are the actual sample point. In the legend 409D represent the downstream and 409U the upstream flow.

MSS - 20th of April event

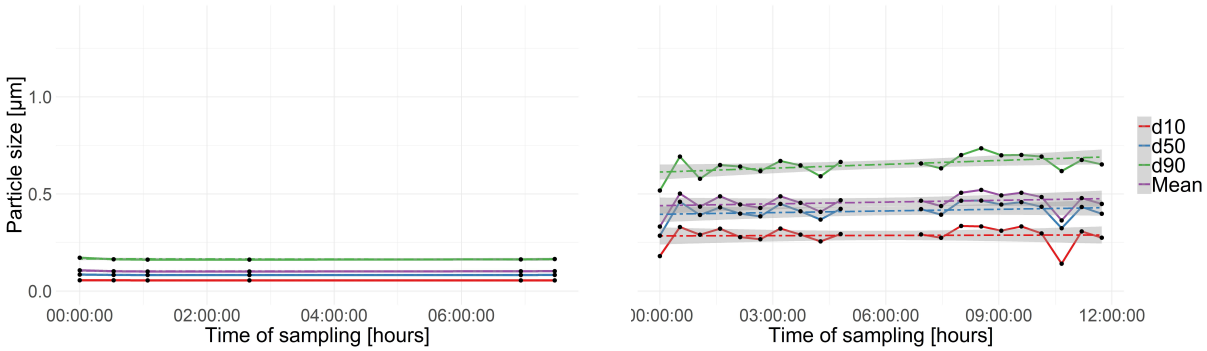

The upstream (left) and downstream (right) plots of the mean, d10, d50 and d90 particles in the 20th of April event. The dotted line represents the trend line.

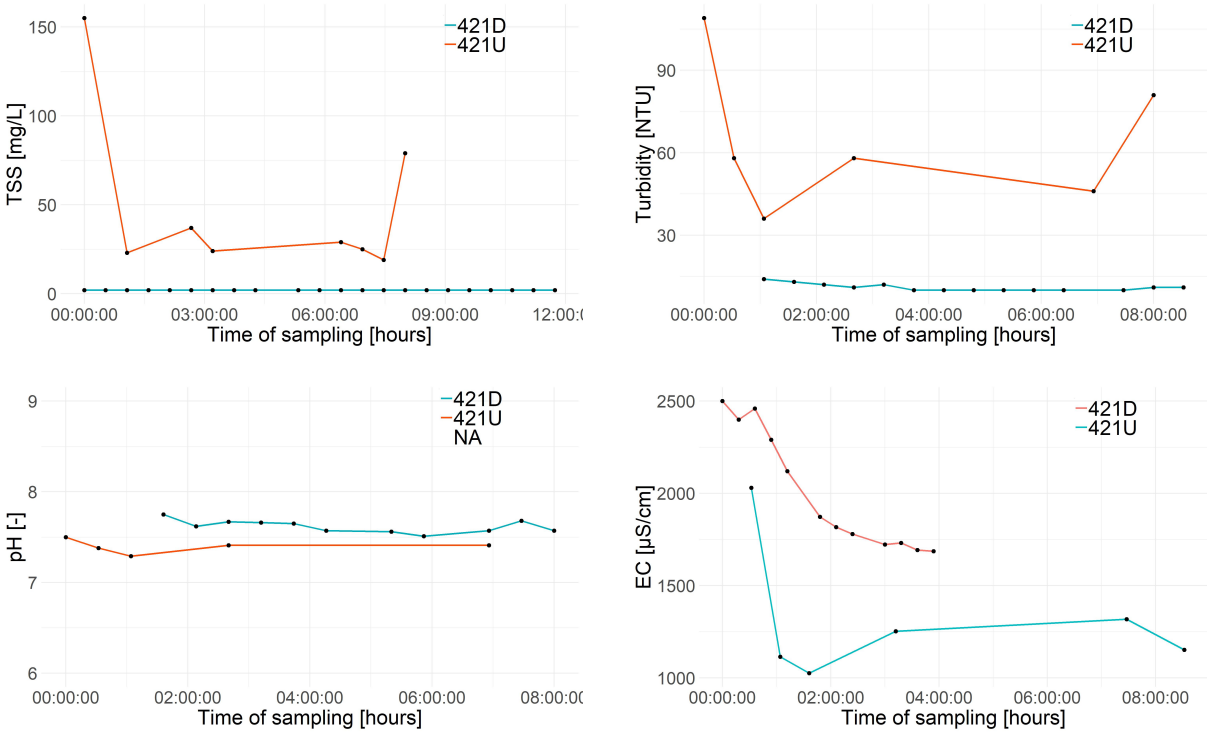

Results of lab analyses for the 20th of April event. The black point are the actual sampling results. In the legend 421D represent the downstream and 421U the upstream flow. All the 421D TSS results are below 2 g/l.

MSS - 9th of May event

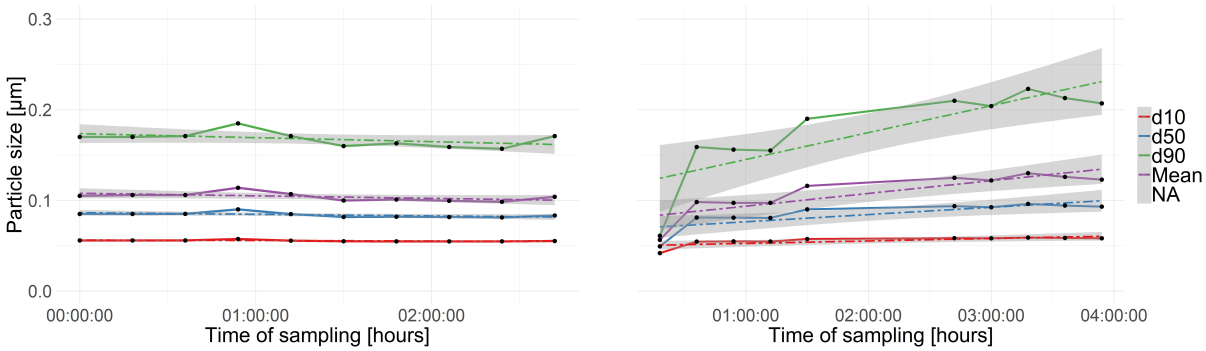

The upstream (left) and downstream (right) plots of the mean, d10, d50 and d90 particles in the 8th of April event. The dotted line represents the trend line.

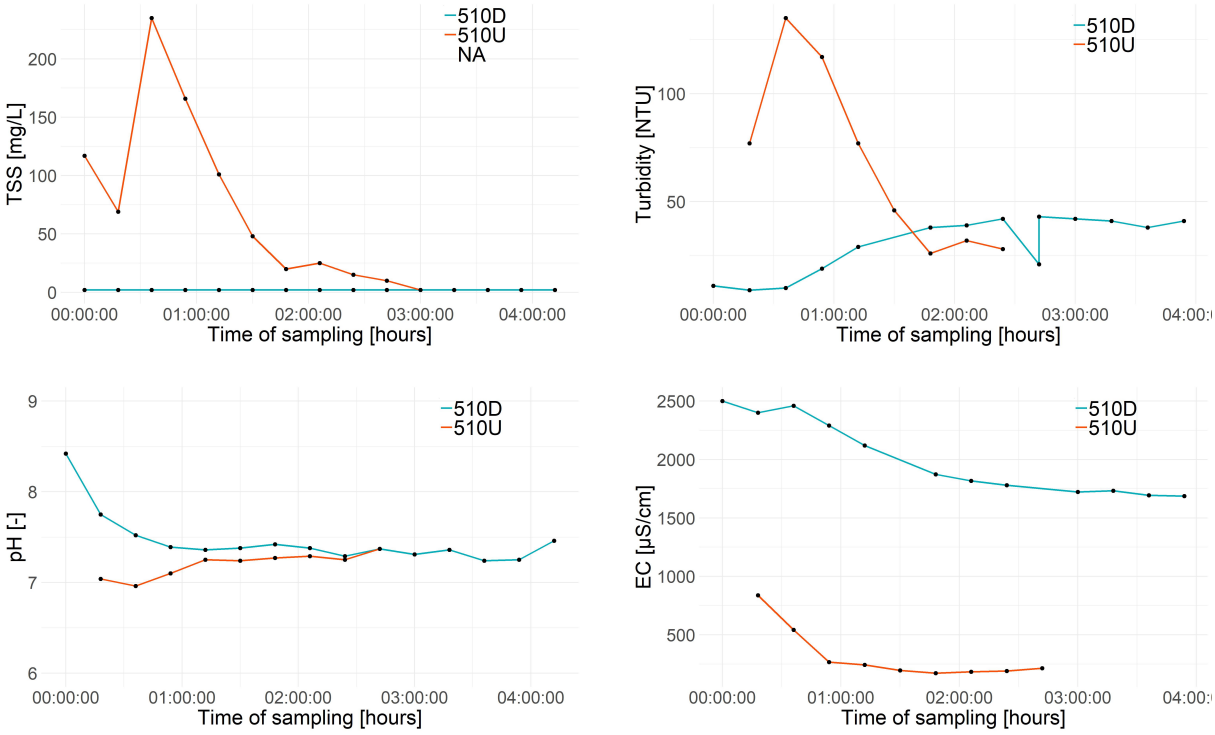

Results of lab analyses for the 9th of May event. The black point are the actual sampling results. In the legend 510D represent the downstream and 510U the upstream flow. All the 510D TSS results are below 2 g/l.

Removal efficiencies

The summarised removal efficiencies for metals and total suspended solids (TSS) of all events are presented in the tables below.

The removal efficiency of Ni, Cu, Zn, Cd, Pb and TSS for each of the five events at the HVS.

		Removal efficiency in event [%]				
Parameter	Fraction	25.02	06.03	20.03	22.03	21.04
Ni	Total	40	-2	49	-	53
	Particle	41	1	-	-	-
	Dissolved	-4	-6	2		8
Cu	Total	35	-68	6	-	74
	Particle	38	-42	-13	-	-21
	Dissolved	11	-135	16	-	66
Zn	Total	40	3	1	-	49
	Particle	41	16	-3	-	49
	Dissolved	16	-29	8	-	48
Cd	Dissolved	29	-35	7	-	16
Pb	Total	39	12	6	-	68
	Particle	39	12	4	-	70
	Dissolved	-13	3	35	-	31
TSS	Particle	40	25	10	2	88

The removal efficiency of Ni, Cu, Zn, Cd, Pb and TSS for each of the three events at the MSS.

		Removal efficiency in event [%]		
Parameter	Fraction	08.04	20.04	09.05
Ni	Total	-	77	52
	Particle	-	63	55
	Dissolved	9	88	48
Cu	Total	-22	77	42
	Particle	-48	47	42
	Dissolved	18	85	42
Zn	Total	7	64	55
	Particle	-20	44	33
	Dissolved	20	71	62
Cd	Dissolved	24	47	-25
Pb	Total	-16	57	55
	Particle	-17	58	60
	Dissolved	1	48	-99
TSS	Particle	48	92	98

F Appendix F - Precipitation and runoff data

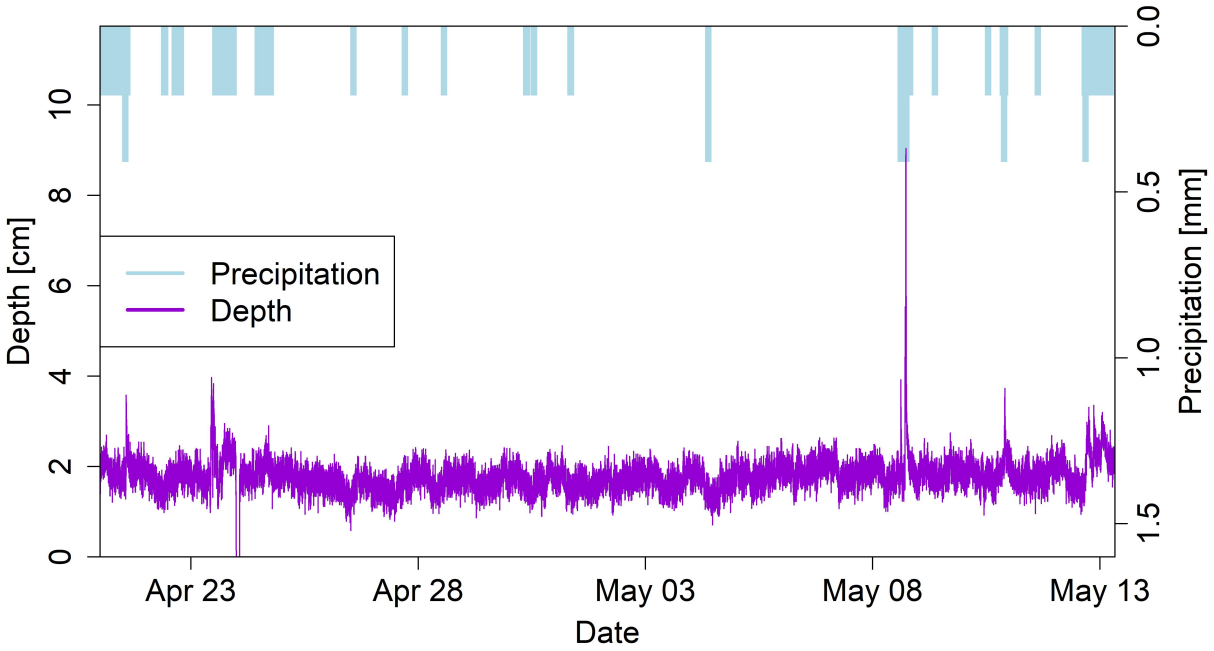

The recorded precipitation from the ECH20 and depth of the upstream diver used for the calibration of the Storm Water Management Model (SWMM).

G Appendix G - Summary of lab analyses of sediments

Summary of the lab analyses of the sediment samples. The particle size distribution are given for the samples with (DIS) and without (NAT) dispersant.

Type	Particle size [μm]	Gully pot				
		818	820	821	829	831
NAT [a]	<50	67	60	62	48	39
	50 - 75	5	6	6	5	5
	75 - 100	3	4	4	4	4
	100 - 150	4	6	5	6	7
	150 - 250	5	8	7	13	12
	250 - 500	7	10	9	13	18
	500 - 1000	5	5	5	7	11
	1000 - 2000	3	2	3	3	5
DIS [a]	<50	60	65	54	53	65
	50 - 75	6	4	5	5	4
	75 - 100	4	3	4	4	3
	100 - 150	6	5	6	6	5
	150 - 250	6	8	8	9	8
	250 - 500	9	9	12	13	9
	500 - 1000	6	4	7	7	4
	1000 - 2000	3	2	5	3	2
PSD of the particles < 50 μm						
PSD, NAT [μm] [b]	D_{10}	0.0587	0.0580	0.0590	0.0594	0.0588
	D_{50}	0.0936	0.0914	0.0949	0.0971	0.0941
	D_{90}	0.199	0.191	0.210	0.227	0.204
PSD, DIS [μm] [b]	D_{10}	0.0619	0.0583	0.0602	0.185	0.0611
	D_{50}	0.106	0.0927	0.0993	0.311	0.0991
	D_{90}	0.264	0.203	0.234	0.682	0.234
Organic matter						
Organic matter [%]	<50 μm fraction	10.0	11.3	9.47	7.23	8.41
	total fraction	7.25	6.51	7.63	3.92	3.95

[a] Differential weight [%] [b] Based on differential number percentage

Pictures from lab analyses of sediment samples.

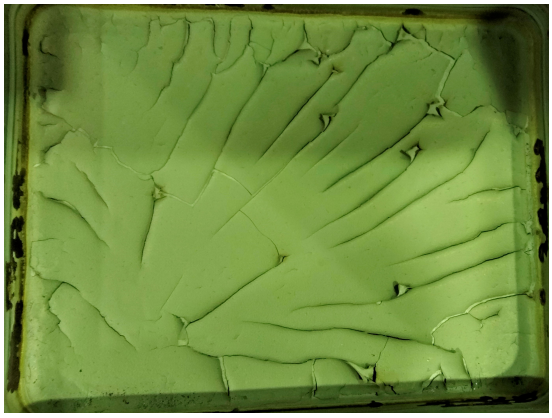

(1)

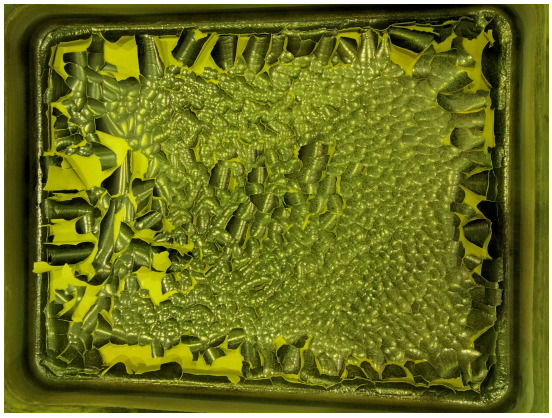

(2)

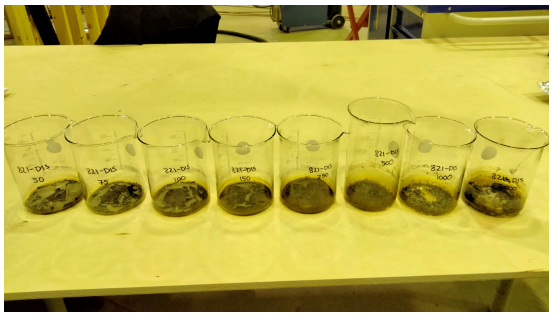

(3)

(4)

Pictures from the analyses of the sediment samples from E6.

(1) The dried <50 μm fraction of the 818 sample without dispersant.
(2) The dried <50 μm fraction of the 818 sample with dispersant. A film of oil can be seen on the top.
(3) Picture of the dried fractions from 50 μm to over 2000 μm.
(4) 100 mL plastic cups with the 831 sample with DIS to the left and NAT to the right. The picture is taken after the cups have been untouched for five days. The NAT sample has sedimented, while in the DIS sample many particles are still in suspension.

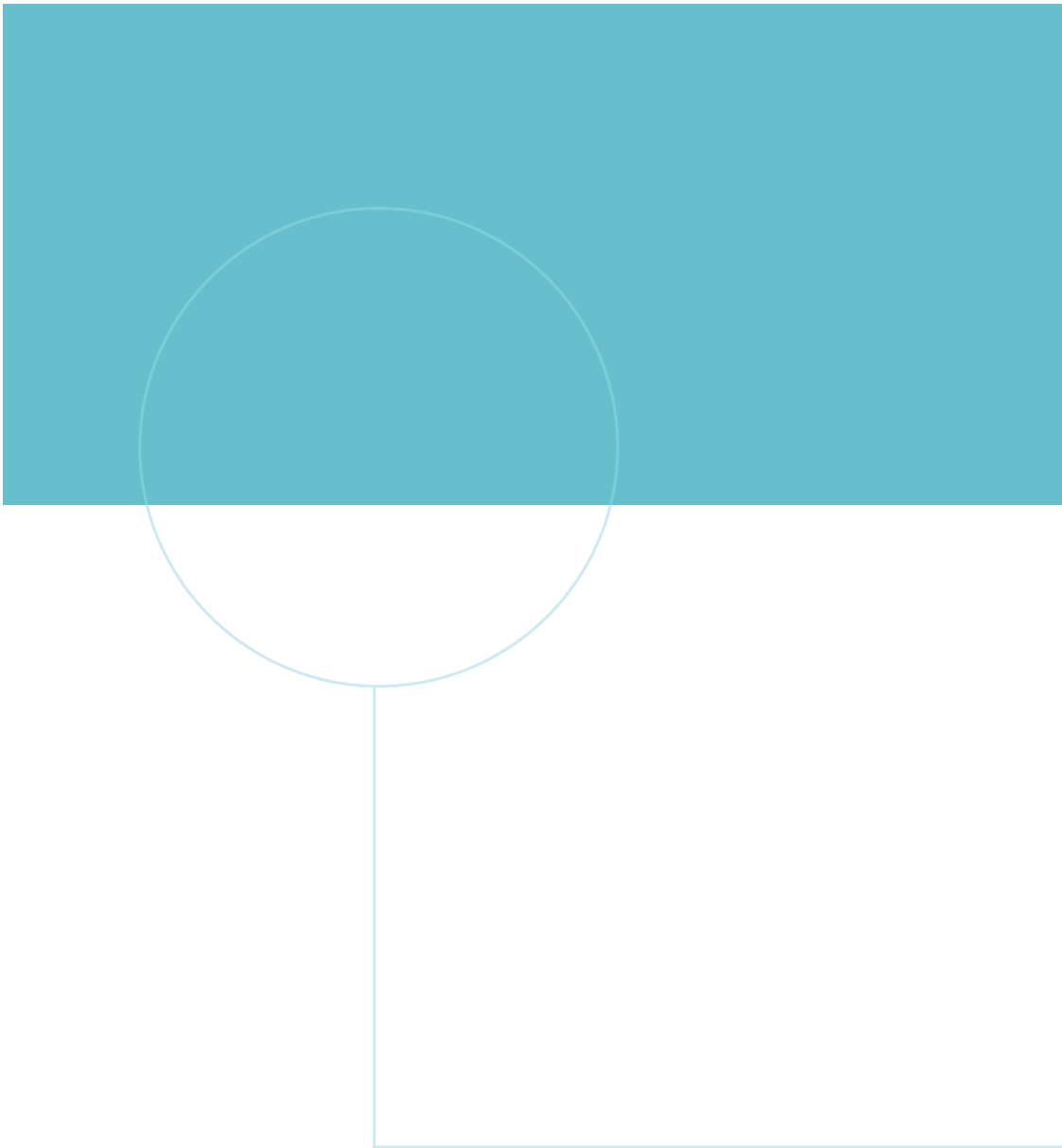

NTNU

Norwegian University of
Science and Technology